24. SYNTHESIS OBSERVING STRATEGIES— A "HITCH-HIKER'S GUIDE"

ALAN H. BRIDLE

1. INTRODUCTION

Many of the previous lectures emphasize problems that can corrupt or distort the images made by synthesis radio telescopes under real conditions. By now, it may seem to you that so many effects can degrade synthesis images that good results must depend on a mixture of luck and magic. I will try to counteract this by describing an orderly way to choose the parameters of radio synthesis observing to avoid at least *some* of the pathological image defects emphasized earlier. I will suggest how to use the material of Lectures 2, 5, 6, 7, 8, 9, 12 and 13 to choose critical parameters when planning synthesis observations. As there is at least one orderly approach to the problem, my first advice is—"DON'T PANIC!" (Adams 1979).

The general principles of this lecture apply when planning observations with any synthesis radio telescope. Figure 24–1 summarizes the approach that I suggest, as a "decision tree" for continuum observers. Sections 2 to 5 describe details of this tree. Section 6 outlines a similar tree (Figure 24–2) for spectroscopy, and Section 7 discusses calibration strategy. Section 8 describes what (little) can be done while the data are being taken. Many details relevant to the NRAO's VLA are contained in an Appendix. This Appendix also has short sections on preparing VLA observing proposals and on PC software (available from the NRAO) that can assist planning for VLA observing.

2. RESOLUTION, BASELINE RANGE AND OBSERVING FREQUENCY

2.1. Resolution $\theta_{\rm HPBW}$ – how much is enough?

The first step is to determine the *range* of resolution $\theta_{\rm HPBW}$ that is appropriate for the project. You should think about both the minimum and maximum values of $\theta_{\rm HPBW}$.

The lowest resolution (*maximum* value of the synthesized beam width $\theta_{\rm HPBW}$) will be set by your need to separate, or to resolve, astrophysically important features of the region being imaged. Realize however that you can have *too much* resolution if your project depends on imaging *extended* emission. There is no point observing extended emission using such a small beamwidth $\theta_{\rm HPBW}$ that crucial features are close to, or below, the r.m.s. noise ΔI_m on the final images. You must therefore estimate the *apparent brightness* (flux density per synthesized beam area) that you expect important extended features to have at the resolution you will use for your final images. You can then determine the highest resolution (*minimum* $\theta_{\rm HPBW}$) that is appropriate for your project by estimating the total integration time $t_{\rm int}$ needed to reach the required brightness

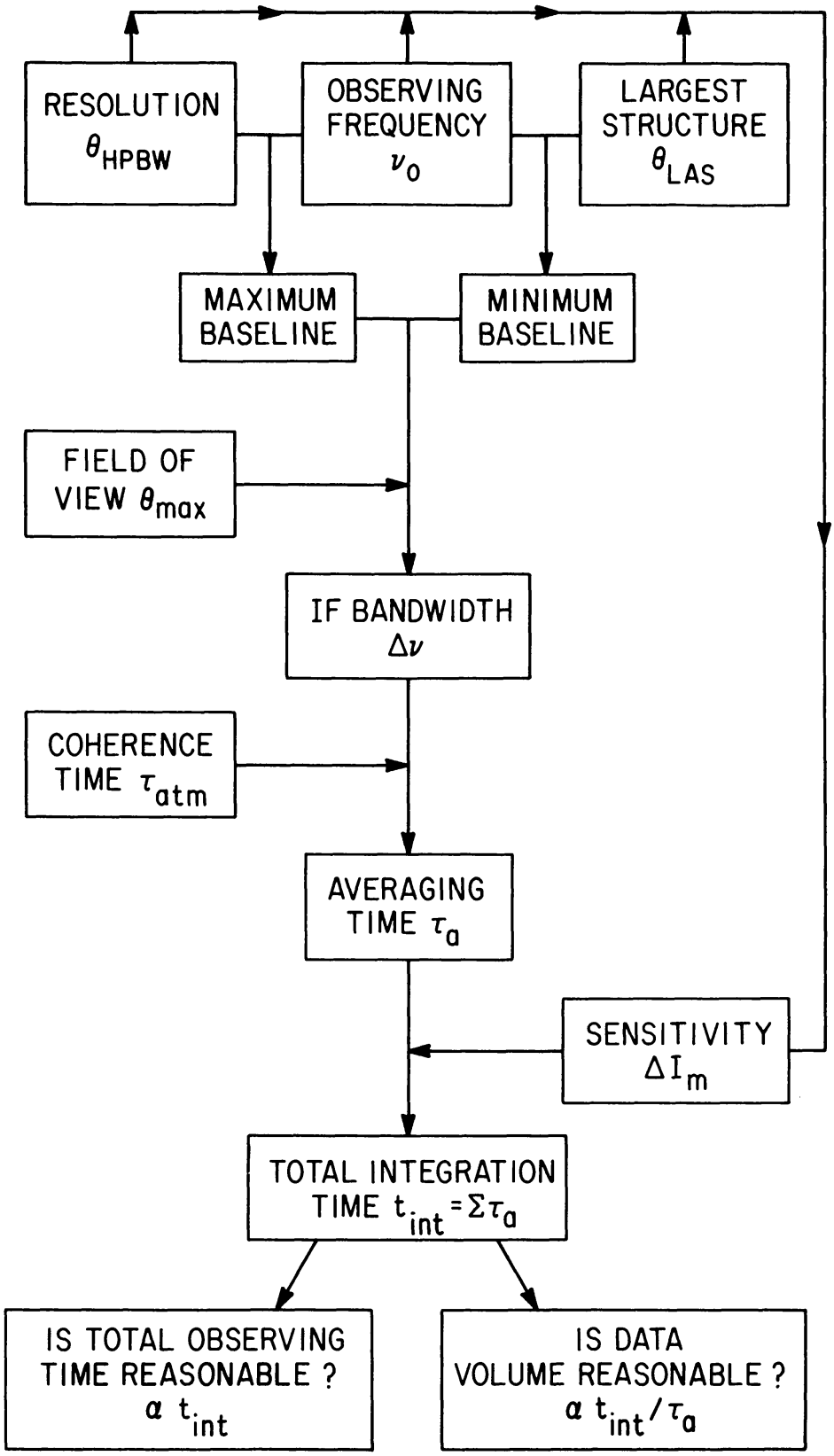

Figure 24–1. Factors Entering Into Continuum Observing Strategy—A Suggested Decision Tree.

sensitivity. As omitting this aspect of the project design can render the final images useless, it is worth restating the principles.

Recall from Lecture 7 that a *point* source with flux density S Jy images with an apparent brightness of S Jy per synthesized beam area regardless of the area Ω_s of the synthesized beam. It follows that, for any synthesis array of identical antennas and receivers, all baselines are equally sensitive to a given point source (apart from the effects of confusion and phase stability). In contrast, as described in Lecture 7, the apparent brightness of an *extended* emission region in a synthesized image depends on the region's detailed structure, on how well the visibility function $V(u, v)$ is sampled by the observations, and on the weighting and tapering functions D_k and T_k applied to the data when imaging (Lecture 6). When deciding on an observing strategy, it usually suffices to assume that:

(a) an extended region with uniform true brightness I Jy per arcsec^2 will be imaged with an apparent brightness $\approx I\Omega_s$ Jy per synthesized beam area, and

(b) the *final* synthesized beam will be a Gaussian 'CLEAN' beam, so that its area Ω_s will be $\approx 1.13\theta_1\theta_2$ arcsec^2, where θ_1 and θ_2 are the major and minor half-power widths of the Gaussian in arcsec.

If the r.m.s. noise on the image is ΔI_m Jy per synthesized beam, the signal-to-noise ratio of such extended emission on the image will be $\sim I\Omega_s/\Delta I_m$, which increases as the synthesized beam area Ω_s. You must ensure that you do not observe at such small values of Ω_s that interesting extended structure is undetectable, given the total integration time $t_{\rm int}$ available and your choice of the IF bandwidth $\Delta\nu$ (see Sections 3 and 4 below).

There are circumstances however when enhanced resolution helps you to detect interesting features—for example, when searching for pointlike "hot spots" or linear "jets" in more diffuse emission such as large scale "lobes". While the flux density per synthesized beam of two-dimensional emission is roughly proportional to the beam *area* Ω_s, that of linear emission is proportional to the beam *width* $\theta_{\rm HPBW}$, and that of a point source is *independent* of beam size. These dependencies allow compact structure that is embedded in, or confused with, more extended emission to be recognized most easily on high-resolution images.

Note that it is also important to avoid unnecessarily high resolution (long baselines) in detection experiments. Although the *theoretical* sensitivity to a point source is independent of the size of the array (apart from the effects of confusion), the phase fluctuations produced by atmospheric irregularities will be greater on longer baselines (see Lecture 5, Section 4.3). It is therefore more difficult to reach the theoretical sensitivity by integrating coherently between calibrations when using long-baseline arrays. This is especially true at high frequencies, where the phase stability depends critically on conditions in the troposphere over the array. The severity of ionospheric or tropospheric phase fluctuations varies from site to site, and at any one site with the "weather" from hour to hour, from day to day, and from season to season. It is generally true however that observations longer than about an hour with $\theta_{\rm HPBW} < 1''$

are often corrupted by atmospheric phase fluctuations and that observations with $\theta_{\rm HPBW} < 0\farcs1$ *always* are. The most powerful tool for dealing with these corruptions is self-calibration (Lecture 9). This technique is rarely applicable to detection experiments, however.[1]

2.2. Largest angular scale $\theta_{\rm LAS}$.

The next step in planning your observations involves thinking about $\theta_{\rm LAS}$, the largest angular scale of structure that you must sample well to produce a useful final image. $\theta_{\rm LAS}$ will be the angular diameter of the most extended structure that you must image accurately—usually the diameter of the most extended component of astrophysical interest in your target. (Do not confuse it with $\theta_{\rm max}$, the required field of view, which is discussed below—when observing a target $10''$ in extent in the presence of a point confusing source $1'$ away, you would set $\theta_{\rm LAS} = 10''$, not $\theta_{\rm LAS} = 1'$.) $\theta_{\rm LAS}$ will set the *shortest* baseline length that must be present in your data for the resulting images to be useful.

The visibility of a circular Gaussian source with FWHM $\theta_{\rm LAS}$ falls to half of its peak amplitude at a normalized baseline length of $91{,}000/\theta_{\rm LAS}$ wavelengths, if $\theta_{\rm LAS}$ is in arc seconds. You will not be able to image a two-dimensional structure of size $\theta_{\rm LAS}$ well unless *projected* baselines at least this short are present in the data. Depending on the density of tracks in the inner u-v plane, and on the sensitivity per baseline, more conservative criteria may be needed—halving the above estimate gives a baseline on which the visibility falls to about 85% of its peak. Note also that the detailed array geometry, target declination and hour-angle range determine how baselines are foreshortened by projection. The most reliable approach is therefore to look at u-v plots for your expected antenna layout, declination, and hour-angle range,[2] to ensure that your planned short-baseline coverage meets the requirements imposed by $\theta_{\rm LAS}$.

The factors affecting the choice of resolution cannot be estimated reliably in advance if the source structure is poorly known. If you are not sure what your source will look like, the safest strategy is to guess on the side of low resolution when designing an initial observation. A "diagnostic" low resolution image may tell you the source's total angular extent, and warn you about surrounding emission. This information will let you optimize the parameters for a more time-consuming high resolution study. It is also easier to justify reobserving a detected emission region at high resolution than to justify reobserving at low resolution what previously appeared to be empty sky!

2.3. Choice of frequency ν_0 at given resolution $\theta_{\rm HPBW}$.

Continuum observers will choose the observing frequency *at a given resolution* by balancing astronomical criteria against instrumental performance. A high frequency may be necessary for polarimetry because Faraday effects decrease with increasing frequency (degrees of linear polarization are generally higher at higher frequencies and electric vectors lie closer to their intrinsic position angles). Polarimetric data are also less corrupted by the Earth's ionosphere at

[1] Unless they are unusually successful, so that all detected sources are strong!

[2] This can readily be done for any antenna array using the program 'UVSIM' in the NRAO's Astronomical Image Processing System.

high frequencies. Studies of Faraday effects (e.g., depolarization) in continuum sources may demand low observing frequencies, however. The spectral index of the continuum also influences the choice of frequency—optically thick thermal emission may be easier to detect at high frequencies whereas transparent synchrotron sources will be easier to detect at low frequencies.

If a continuum project has frequency agility, the choice of ν_0 also involves the receiver sensitivity and antenna performance as a function of frequency. High frequency observations are often limited by worsening receiver noise performance, antenna efficiency and pointing accuracy (as a fraction of the primary beam size) with increasing frequency. Low frequency observations are limited by interference at many radio observatories.

a) Interference.

The detailed choice of observing frequency, especially below 2 GHz, is often constrained by known sources of radio frequency interference (RFI). For example, U.S. frequency allocations in the L Band around 20 cm include aeronautical radio navigation (including global satellite networks), meteorological aids, and fixed and mobile use. Many of the possible external interfering signals are time variable, so freedom from external interference can never be guaranteed at L Band outside the protected radio astronomy bands. The protected band from 1400 to 1427 MHz is undesirable for some continuum observations, however, because galactic neutral hydrogen emission can increase the system temperature significantly in this band.

External interfering signals are partially rejected by interferometers (e.g., Thompson 1982a) because only the component of the signals that (a) varies at the sidereal fringe rate, and (b) correlates with the correct delay, will affect the output. In practice, this combination makes low frequencies and short-baseline synthesis arrays more sensitive to RFI than high frequencies (where radio frequency band allocations are less congested) and long-baseline arrays.

Data averaging reduces the response to interfering signals by the factor $\mathrm{sinc}(\nu_f \tau_c)$ where ν_f is the natural fringe frequency and τ_c is the time over which the data are averaged when computing the visibility in each u-v cell before Fourier transforming. As $\nu_f = \omega_e u \cos\delta$, where ω_e is the angular velocity of the Earth's rotation and δ is the declination, fringe rate rejection is least for observations near the celestial poles and for baselines near the v-axis, where fringe frequencies are near zero. In a given RFI environment, long-baseline arrays collect more data at large values of u than do short-baseline arrays, so long-baseline arrays are less affected by RFI (unless the RFI is strong enough to degrade the noise performance of the individual receivers). Short-baseline arrays may also suffer more from locally-generated RFI or from "crosstalk" (correlations between signals radiated by the electronics of one antenna directly into the feed or the electronics of another).

Delay rejection is a more complex function of the azimuth of the baseline and the position of the interfering source, as described in detail by Thompson (1982a). Its effects cannot be stated as concisely as those of fringe rate rejection and are not a simple function of location in the u-v plane. Delay rejection is not

usually significant for narrow-band interfering signals.

RFI may always be edited from the data after they are taken (with particular attention to data falling near the v-axis), but careful choice of observing frequency can minimize both the effort necessary for editing and the consequent loss of data.

b) Imaging at more than one frequency.

When studying spectral index, Faraday rotation or depolarization properties of extended sources, you should attempt to minimize uncertainties arising from differing resolutions at the different frequencies. It is important to try to "scale" the distributions of baseline lengths in *wavelengths* that are used for the different observations. Ideally, you would scale the detailed distribution of antenna spacings but it is often difficult to scale more than the inner and outer baseline limits and the tapering and weighting functions (especially when observing with fixed arrays, as in VLBI). You should also make the hour-angle ranges of the observations at different frequencies as similar as possible.

Note that although using such "scaled arrays" *optimizes your chances* of measuring frequency-dependent properties of a source accurately, it cannot *guarantee* success. Even scaled arrays may have significantly different relative sensitivities to different scales of structure if the structure changes radically with frequency, e.g., if there are large spectral index gradients in either the total or polarized emission. You must also be careful when interpreting the final images if the databases at different frequencies are differently affected by missing antennas or by bad data. In many cases, the reliability of inter-frequency comparisons depends on how well the deconvolution algorithm (Lecture 8) interpolates unsampled parts of the u-v plane, even when scaled arrays have been used.

Observing at several adjacent, but not necessarily contiguous, frequency bands can improve the u-v coverage, and so help you to reconstruct complex structures with high fidelity, by "bandwidth synthesis" (see Lecture 12). For this application, observing frequencies should be spaced to minimize the sizes of residual "holes" in the u-v coverage. For example, if the largest "holes" $\Delta u, \Delta v$ in the coverage at one frequency are about 10% of the corresponding radii $\sqrt{u^2+v^2}$, data from two observing frequencies separated by 5% might be combined.

3. Field of View Restrictions

Once you have settled on the resolution θ_{HPBW}, baseline range and observing frequency ν_0 for your program, the next decision (see Fig. 24–1) involves IF bandwidth $\Delta\nu$ and averaging time τ_{a}. These must be consistent with the field of view requirements of your program. You must therefore consider the radius θ_{max} (from the center of the field of view) over which you require the data to be minimally distorted by chromatic aberration and time-average smearing as discussed in Lectures 2, 12 and 13.

3.1. IF bandwidth $\Delta\nu$.

An unsuitable choice of the IF bandwidth may lead (a) to irrecoverable distortion of the image by chromatic aberration if the bandwidth is too great

(see Lectures 2, 12 and 13) or (b) to unacceptably low sensitivity if it is too small.

As discussed in detail in Lecture 13, images made with finite bandwidth are degraded away from the delay tracking center by radial smearing and reduction in amplitude of the point source response. The first step in choosing the IF bandwidth for continuum work is therefore to ask over what field radius $\theta_{\max}$ (arcsec) you require that these chromatic aberration effects be limited to broadening the beam by $< n\%$ or to reducing the amplitude of a point source by $< m\%$. Then obtain the corresponding value $\beta_{\max}$ of the normalized parameter β, either from the graphs shown in Figures 13–1 and 13–2, or from Equations 13–19, 13–24 and 13–29. The maximum allowable IF bandwidth $\Delta\nu_{\max}$ (MHz) consistent with these constraints is then given by

$$\Delta\nu_{\max} = \frac{\beta_{\max}\nu_0\theta_{\mathrm{HPBW}}}{\theta_{\max}}, \qquad (24\text{–}1)$$

where ν_0 is your observing frequency in MHz and θ_{HPBW} is the half-power beamwidth in arcsec at which you expect to make your images. Unless you are prepared to relax your smearing/attenuation criterion slightly, select the closest allowed bandwidth that is *narrower* than $\Delta\nu_{\max}$. If you are prepared to relax it, choose the closest *wider* bandwidth.

Your choice of $\theta_{\max}$ may be determined by the need to image an extended structure with minimal distortion, or by the need to include a strong confusing source in the minimally-distorted field of view. The latter need arises because you may wish to subtract or deconvolve a confusing source's sidelobes from the interesting region. The value of $\theta_{\max}$ will always be greater than, or about equal to, the value of θ_{LAS} used earlier when selecting the range of baselines. In general, choose the delay and pointing center to minimize the required $\theta_{\max}$ for your observations. When using a wide field to include a confusing source, consider displacing the delay center away from the target towards the confusing source. This will avoid the use of unnecessarily narrow bandwidths (and thus of unnecessarily low sensitivity). If the field is *dominated* by a strong point source (more than ten times brighter than other structure), *this* source should be placed near the delay center and pointing center when high dynamic range is required. This strategy will minimize the total distortion of the image resulting from bandwidth, pointing, averaging time and computational effects (such as u-v truncation) involving the strong source (for more details, see Clark 1981).

For point source detection experiments the above criteria will normally select the widest available bandwidth, unless the search position is exceptionally inaccurate or the field is known to be highly confused. Chromatic aberration affects observing strategy less critically at higher frequencies for several practical reasons—fractional bandwidths ($\Delta\nu/\nu_0$) are often smaller; the usable field of view is limited by the primary HPBW of the antennas for the narrower fractional bandwidths; receiving systems are noisier and antennas are less efficient (so sensitivity, not distortion, limits image quality).

When deciding on the value of $\theta_{\max}$ that is appropriate for an image of an extended source, consider the detectability of the extended emission *at the*

resolution you will be using for your images (see Sections 2 and 4). There is no point ensuring that extended structure is not smeared radially by the bandwidth effect if low signal-to-noise on the same structure introduces uncertainties larger than the bandwidth distortions. As the signal-to-noise on extended emission itself depends on the choice of IF bandwidth, this calculation may need to be iterated until a suitable compromise is reached.

3.2. Visibility averaging time τ_a.

It is important to choose the "on-line" averaging, i.e., averaging applied to the data before they are written to an initial storage medium, carefully. The data will be averaged relative to a particular phase tracking center and this on-line averaging cannot be undone. Any excess averaging done off-line, after the data have been archived, can be undone later, though it is obviously inefficient to do this.

The effects of finite averaging time τ_a were outlined in Lectures 2 and 12 and discussed in detail in Lecture 13. As τ_a is increased, phase winding of a point source at radius θ from the phase center both smears and attenuates the synthesized response to such a source. The effect is worst on a given baseline when Earth rotation moves the source perpendicular to the fringes associated with that baseline, but is zero when the feature moves parallel to the fringes. The magnitude of the effect therefore depends on baseline orientation, hour-angle and declination, as described in Lecture 13 by Equations 13–31, 13–35, 13–36 and 13–37. For an array observing a point source near the north celestial pole, the *average* reduction in amplitude can be estimated from Equations 13–41 to 13–43, provided the reduction is small. Restating those results, the average reduction in amplitude of a polar point source θ from the phase tracking center is given by

$$\overline{\langle R_\tau \rangle} = \frac{I}{I_0} = 1 - \eta \left(\frac{\theta}{\theta_{\mathrm{HPBW}}} \right)^2 \tau_a^2 , \qquad (24\text{–}2)$$

where $\eta = 1.05 \times 10^{-9}$ for uniform square u-v coverage, $= 1.08 \times 10^{-9}$ for uniform circular coverage and $= 1.22 \times 10^{-9}$ for circular, Gaussian tapered, coverage. τ_a is in seconds.

The choice of τ_a balances several issues. First, you must decide what amplitude reduction R_τ due to time-average smearing will be acceptable at $\theta = \theta_{\mathrm{max}}$. Then estimate the corresponding τ_a from Equation 24–2 using appropriate values of η and θ_{HPBW}. If sensitivity or hardware considerations force you to choose an IF bandwidth that is wider than the $\Delta\nu_{\mathrm{max}}$ given by Equation 24–1, estimate τ_a so that the effects of time-average smearing at θ_{max} are slightly less than those of chromatic aberration. (See the Appendix, Section A4, for an example.)

Ideally, you would observe with τ_a set to the value estimated from Equation 24–2 unless this exceeds the expected coherence time τ_{atm} for the atmospheric phase fluctuations on the longest baselines, or unless it is too long to let you edit the data satisfactorily. In either of those cases, you would observe with a shorter τ_a. You would later average the edited, calibrated data to the value estimated from Equation 24–2, to minimize the data volume and the image processing time. In the real world, constraints on computing resources (storage

space and CPU time) may force you to use longer averaging times than would be desired purely for image quality.

4. Total Integration Time $t_{\rm int}$

Once you have determined the IF bandwidth $\Delta\nu$ from the field of view criteria, the next step in the decision tree (Fig. 24–1) is to estimate the total on-source integration time $t_{\rm int}$ required for given sensitivity on your final image. Here you will use the expression for the r.m.s. noise ΔI_m on an image made with an N-antenna array:

$$\Delta I_m = F_{\rm w}\Delta S \Big/ \sqrt{\frac{nN(N-1)}{2} t_{\rm int}\Delta\nu}\ , \qquad (24\text{–}3)$$

where n is the number of independent IFs contributed to the image per antenna ($n = 2$ for images of Stokes I from two orthogonal polarization states at one sky frequency, or for images of $P = \sqrt{Q^2 + U^2}$ at one sky frequency), $t_{\rm int}$ is in seconds, and $\Delta\nu$ is in MHz. In the numerator, $F_{\rm w} = 1.0$ for natural weighting and is > 1 for other weightings (the value depending on the gridding and on the baseline distribution—see Lecture 7 for details). ΔS is the single-interferometer sensitivity per second per MHz of IF bandwidth.

The sensitivity goal will be determined by (a) the significance level you need for a detection to achieve your astronomical goals, and (b) whether the interesting emission is extended (see Section 2.1 above). If you are doing polarimetry, calculate the sensitivity from the expected *polarized* intensity, not total intensity.

If the first estimate of $t_{\rm int}$ is significantly greater than 12 hours, consider carefully whether your choices of frequency and baseline range are optimal. You may wish to re-enter the decision tree with different starting parameters before considering the proposal planning further.

If you estimate $t_{\rm int} < 4$ hours, your observing strategy should be determined by the need for dynamic range and by whether you can merge observations of several sources into one program. If you require high dynamic range, or wish to image an extended structure, with less than a full synthesis you should sample the u-v plane as uniformly as possible. This can usually be done satisfactorily by distributing the observing over several short (e.g., $\sim$ 10-minute) scans spaced equally through the available hour-angle range. Note however that the dynamic range achieved in a given observation also depends on atmospheric and ionospheric conditions, on the elevation angle range, and on your calibration strategy (Section 7 below), as well as on the u-v coverage.

Two-dimensional arrays with many antennas may have good enough instantaneous u-v coverage to make a "snapshot" mode attractive for observations of strong, compact sources when the total integration time required is small. The Appendix (Section A7) discusses the advantages and disadvantages of snapshot mode.

5. Confusing Sources

Confusion may have two effects on the interpretation of a synthesis image:

(1) the r.m.s. fluctuation level on the image may be degraded by sidelobes or by aliasing of confusing sources, and

(2) an extraneous radio source may be mistaken for the target in a detection experiment, or considered part of the structure of an extended feature.

The best way to handle confusion is to *learn about it* in the context of your particular target field. Before you observe, consult published radio surveys, or low resolution images of the field around your target, for possible confusion. If you know you will be observing near a bright confusing source, you may consider either of two strategies for reducing its effects on your final images.

If the confusion is relatively nearby, plan to look at it—to make wide-field images containing both the target and the confusing source. Then subtract or 'CLEAN' the confusing source and its sidelobes from the interesting region. The ungridded subtraction technique[3] (Lecture 8, Section 1.3) helps this strategy, as only the parts of the wide field that contain significant emission need to be computed and 'CLEAN'ed. This approach can work well if the confusing source is only one or two times as far from the target as the radius of the field of view that you would otherwise have imaged. If the confusing source is strong, consider displacing the delay tracking center away from the target toward the confusion, to minimize distortions of the response to the confusing source by chromatic aberration and other effects.

If the confusion is relatively distant, try *not* to look at it—choose your IF bandwidth and the delay, phase and pointing centers to minimize the response to the confusing source. Note that because the point source attenuation produced by chromatic aberration and time averaging increases with baseline length $\sqrt{u^2 + v^2}$ (see Lectures 12 and 13), these effects do not filter confusing sources from the short-baseline data as effectively as they do from long-baseline data. If a distant confusing source still dominates the data after attenuation by the primary beam, it may therefore produce wide-angle "ripple" in the final image. In such cases, the pointing center should be chosen to minimize the response to the confusion rather than to maximize the response to the target.

A difficult case arises when the response to the confusing source is strong even after adopting this stratagem. Variable pointing errors and (for altitude–azimuth antenna mounts) the rotation of the primary sidelobe pattern of the antennas on the sky may then make the confusing source appear to vary throughout the observation. It is hard to make images with high dynamic range in these circumstances (see also Lecture 12, Section 2.1). It is worth recognizing this difficulty before observing, if only because you might be able to select an alternative target that is equally interesting.

If a confusing source lies in the target field itself, no advance precautions are necessary, as the confusing source and its sidelobe pattern can be deconvolved

[3] coded in the NRAO Astronomical Image Processing System as the program 'MX'.

from the image as part of normal data reduction. Note however that it is important to *look* for confusion *after* taking the data, e.g., by making a heavily-tapered low-resolution image covering as much sky as possible around your target. It is particularly important to do this before proceeding with computer-intensive processing such as deconvolution, or self-calibration at full resolution. Making low-resolution images to search for confusing sources early in your image processing may (a) improve the models used for self-calibration, (b) reveal unexpected large-scale structure around your target (and so help to define 'CLEAN' deconvolution windows) and (c) lead to unexpected discoveries.

In detection experiments, confusion may make the interpretation of a positive detection questionable if a source is detected near, but not at, the target position. Source counts (e.g., Section A9 of the Appendix) should be used to estimate the probability that the detected source lies in the image by chance.

6. Spectral Line Observing

Spectroscopists have to balance slightly different constraints than those confronting continuum observers. Figure 24–2 summarizes an alternate decision tree appropriate for spectral line observing.

6.1. Observing frequency.

Many spectroscopic experiments have little choice of observing frequency. The line frequency is set by the chemical species and transition relevant to the astronomical problem. The observing frequency is then determined by correcting the line frequency for the systemic radial velocity and for the various motions of the Earth (see Lecture 17, Table 17–1). For the experiment to be viable, the corrected frequency must, of course, lie within the tuning range of the receivers and feeds.

If the chemical species has many radio-frequency transitions (e.g., recombination lines), instrumental performance and astronomical criteria may again be combined. For such projects, the instrumental criteria are similar to those for the continuum: receiver sensitivity, antenna efficiency, pointing accuracy. The astronomical criteria may include whether different transitions will be in emission, or absorption, or both.

The last factor to be considered is radio frequency interference (RFI), as described in Section 2.3*a*. Some spectroscopic observations, especially those at frequencies below 2 GHz and those of objects whose red shifts move the observing frequency out of a protected band, are simply not possible because of RFI.

6.2. IF bandwidth.

Two IF bandwidths enter into the observing strategy for spectral line work. The first is the *total* IF bandwidth $\Delta\nu_{\rm tot}$ that is spanned by all the line channels. $\Delta\nu_{\rm tot}$ determines the *range* of velocities included by the experiment, which should span not only the interesting parts of the line profile, but also an adequate number of line-free channels (allowing for any band-edge effects in autocorrelation spectrometers). The second is the individual *channel* bandwidth $\Delta\nu_{\rm ch}$. This sets the velocity *resolution* of the experiment. It also determines the chromatic aberration effects for the individual channel images. As indicated in Figure 24–2,

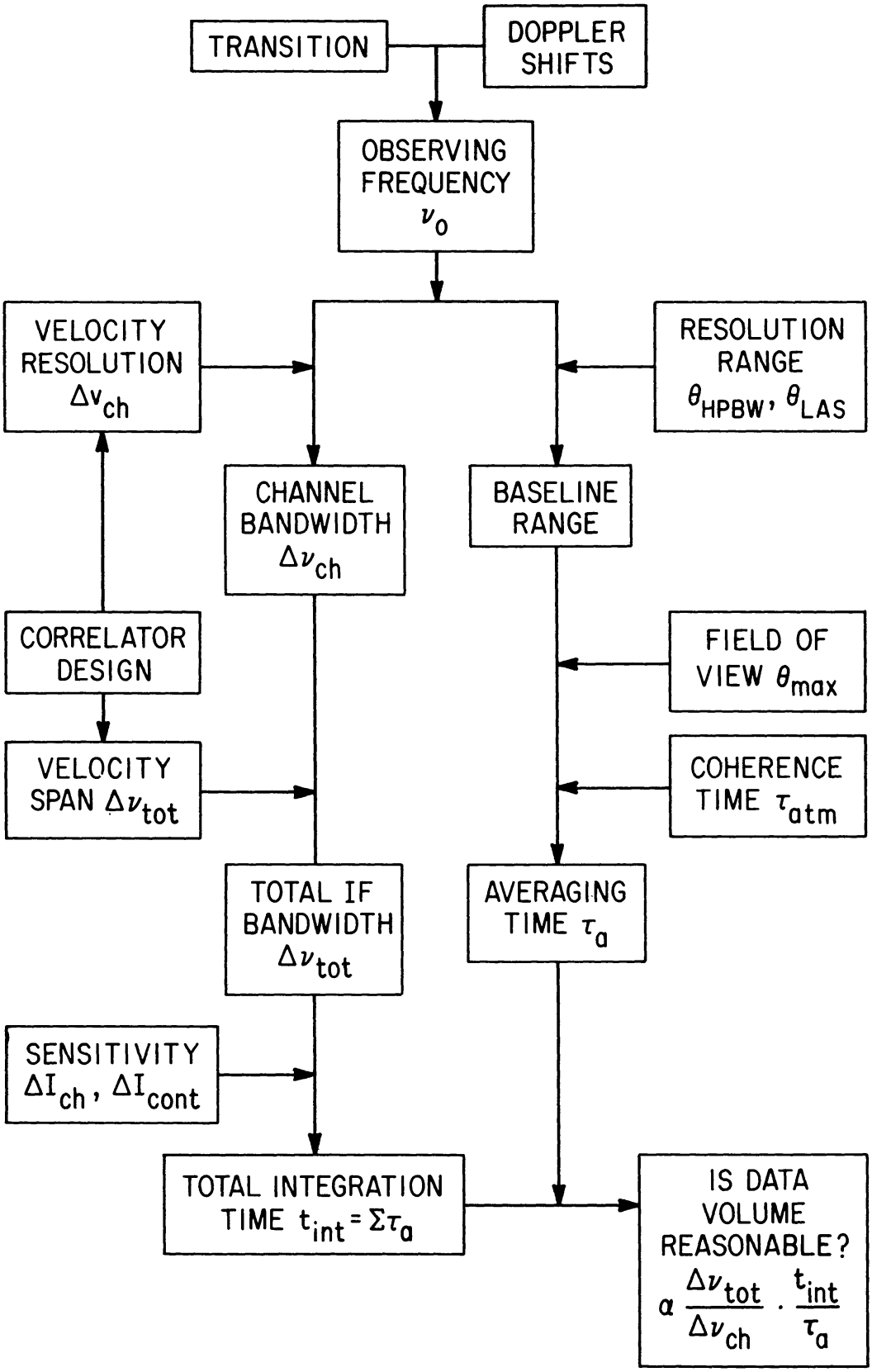

Figure 24–2. Factors Entering Into Spectral Line Observing Strategy—A Suggested Decision Tree.

the choices of $\Delta\nu_{\rm tot}$ and $\Delta\nu_{\rm ch}$ are usually tightly coupled by the design of the spectral line correlator, and velocity resolution and velocity span must often be traded against one another.

The need for velocity resolution usually drives the *channel* bandwidth to a small value so that individual channel images are negligibly smeared by chromatic aberration. This does not mean, however, that spectroscopists can ignore chromatic aberration in synthesis imaging. The *synthesized beam* pattern is different for every channel image when the channels are gridded separately with their correct frequencies. Any data reduction schemes that do not separately deconvolve the synthesized beam from each of the individual channel images may therefore "rediscover" effects related to the frequency dependence of the beam. As Lecture 18 describes, such separate deconvolution of all the channels is not always a good strategy. If you estimate the continuum distribution by summing the "dirty" images over a range of line-free channels, or if you difference two "dirty" line channel images, the variation of the synthesized beam with frequency may become apparent. If you try to avoid this effect for some channels by artificially assigning them the same frequency (to make the "dirty beam" the same for all images), you will restore the chromatic aberration corresponding to the widest channel separation $\Delta\nu_{tot}$ used in such processing.

6.3. Averaging time $\tau_{\rm a}$.

Ideally, the averaging time $\tau_{\rm a}$ for spectroscopy will be determined by considering (a) the distortion produced by time-average smearing (Equation 24–2), and (b) the atmospheric coherence time $\tau_{\rm atm}$. Because narrow-band channel images are relatively free from chromatic aberration, it rarely makes sense to choose $\tau_{\rm a}$ for high-resolution spectroscopy by matching time-average smearing to chromatic aberration, as in some continuum experiments.

In practice, however, observations with narrow channel bandwidths may also require long *total* integration times $t_{\rm int}$ to reach sufficient signal-to-noise in the individual channel images. This interacts with the choice of $\tau_{\rm a}$, because a long averaging time may be needed simply to restrain the number of independently recorded visibilities. If $\tau_{\rm a}$ is limited by the data volume, Equation 24–2 should be used to check the distortion at the edge of the interesting field. If a $\tau_{\rm a}$ that keeps the data volume manageable also produces significant distortion, you may have to balance using (a) long averaging times $\tau_{\rm a}$ (image distortion), (b) wider channel bandwidths $\Delta\nu_{\rm ch}$ (poorer velocity resolution), (c) fewer channels $\Delta\nu_{\rm tot}/\Delta\nu_{\rm ch}$ (poorer velocity span), or (d) fewer antennas N (poorer image quality) to restrain the data volume ($\propto N(N-1) \times (t_{\rm int}/\tau_{\rm a}) \times (\Delta\nu_{\rm tot}/\Delta\nu_{\rm ch})$).

6.4. Sensitivity and total integration time $t_{\rm int}$.

Spectroscopists may need to consider separately two different sensitivities—the sensitivity to spectral features in the individual line channels and the accuracy with which the continuum can be estimated from the line-free channels. The need for individual channel sensitivity normally dominates, however. The calculation uses Equation 24–3, with $\Delta\nu_{\rm ch}$ replacing $\Delta\nu$. It may also be appropriate to express the sensitivity in terms of brightness temperature by converting from mJy per beam area to temperature units assuming a Gaussian beam of area

$\Omega_s = 1.13\theta^2_{\rm HPBW}$.

Use of narrow channel bandwidths $\Delta\nu_{\rm ch}$ often implies that sensitivity, rather than u-v coverage, considerations determine $t_{\rm int}$ for high-resolution synthesis spectroscopy, so that observations > 12 hours long may be needed. Spectroscopic observations may also need long integrations on the calibration sources to achieve enough sensitivity.

6.5. Time of day.

Because spectroscopic experiments commonly use compact arrays and narrow bandwidths, they are more prone than continuum observations to disruption by sidelobe responses to solar radio emission. (Both short baseline lengths and narrow channel bandwidths reduce the immunity from far-out sidelobe responses that stems from bandwidth smearing.) This problem is especially severe at low frequencies and at times of enhanced solar activity. Below 2 GHz, night-time observations may be obligatory for many spectroscopic experiments when the Sun is active.

7. Calibration Strategy

The basic issues to be decided by the observer are: (a) what system-wide parameters will be determined satisfactorily by special purpose calibrations before the observing and (b) what time-dependent calibration parameters will be monitored, and how often, during the observing itself. The first decision will vary from observatory to observatory and from project to project. It must be approached by reviewing all the calibration steps described in Lecture 5, and asking how well each calibration parameter will be known in advance relative to the needs of the project. I concentrate here on the second issue, which itself has two main parts—how often to monitor the instrument and the atmosphere by observing reference sources, or "calibrators", and how close the calibrators should be to the target(s). Your strategy will depend on whether you attempt to calibrate only the instrumental fluctuations, or these fluctuations plus the apparent amplitude and phase variations introduced by the ionosphere and troposphere (again, see Lecture 5 for details). Any calibration that monitors atmospheric fluctuations will, of course, calibrate instrumental fluctuations also.

7.1. Instrumental calibration.

The instrumental calibration should (a) detect grossly malfunctioning antennas so that faults can be corrected while the observations are in progress, and (b) monitor the amplitude and phase stability of the instrument rapidly enough that changes can be corrected by interpolation throughout the run. In a well-designed array, most instrumental fluctuations (apart from phase jumps) are slow, so that observations of an unresolved strong calibrator every few hours or more will monitor the instrument adequately. Bear in mind however that if the instrumental calibration detects a discontinuity such as a phase jump, you may have to discard all the data between consecutive calibration observations for the antenna-IF in which the jump occurred (unless the source being imaged is strong enough that the precise time of the jump can be located in the source data—in which case you can probably self-calibrate it anyway).

Calibrators for purely instrumental monitoring should be chosen primarily for their strength rather than for closeness to the target(s).

7.2. Atmospheric calibration.

It is more important, and much more difficult, to calibrate amplitude and phase fluctuations that result from changes in the propagation properties along the atmospheric path to the target. Unfortunately, *no calibration based on observations of a phase reference source that is not in the same isoplanatic patch as the target can be guaranteed to improve the data quality.* This does not mean that attempts to calibrate atmospheric fluctuations using distant reference sources are a waste of time, but you must recognize that such "external" calibration may or may not be successful.

a) External calibration.

If the target and calibrator are separated by an angle greater than that subtended by the atmospheric cells responsible for the amplitude and phase variations, the fluctuations seen in the calibrator data may not correlate with those in the target data. Corrections interpolated from the calibrator observations into the rest of the data under these circumstances may *worsen* the atmospheric amplitude and phase noise on the target by a factor of $\approx \sqrt{2}$. At the other extreme, if the target and calibrator are typically within the *same* isoplanatic patch, the fluctuations observed in the calibrator will faithfully track those occurring in the target. Amplitude and phase corrections interpolated into the target data from the calibrator data in time series may then greatly improve the quality of the final image. The basic problem is that the scale size of the isoplanatic patch will vary from day to day and even from hour to hour (as a function of the "weather" and of the elevation of your target above the horizon). It is therefore difficult to judge how reliable amplitude and phase referencing from a distant calibrator may be before the observations begin.

If you cannot, or do not wish to, rely on self-calibration to remove atmospheric effects from your data, you should choose external calibrator(s) as close as possible to the target(s), ideally within a degree or so of them. You must then hope that the amplitude and phase stability found in the calibrator data meet the needs of your experiment, and that the scale of the isoplanatic patch is typically greater than the calibrator–target separation.

If the within-scan *and scan-to-scan* amplitude or phase fluctuations on a calibrator a degree or two from your target are small (less than 10% or 20°), it is unlikely that much larger fluctuations are occurring on your target and correcting the rest of the data using long-term averages of the calibrator phases is quite likely to improve matters.

If you see large, rapid fluctuations on the calibrator, you are in trouble, which may or may not be mitigated by correcting the rest of the data by local (point-to-point) interpolation in the fluctuations. Because such interpolation may indeed make matters worse, you might then try making images (a) after long-term averaging, and (b) after local interpolation, of phase corrections from the calibrators. You can then judge empirically which gives better final images—using the final dynamic range, r.m.s. noise level, and/or any prior knowledge

about the source to make your judgment.

Deleting data from some or all baselines during periods of unusually bad phase stability will usually improve the quality of images made by external calibration. Imaging with less data but with good amplitude and phase stability can give better results than imaging with much poorly-calibrated data—if the synthesized beam is closer to the theoretical "dirty" beam, deconvolution algorithms work better, increasing the dynamic range of the images. Note that tapering the u-v data down-weights the visibilities from the longer baselines where phases are less stable. Be ready to sacrifice resolution in favor of forming the theoretical beam more closely when the phases are unstable, if your astronomical goals can be met at lower resolution.

Observers doing detection experiments are usually forced to use external calibration. Fortunately, they do not usually require such high dynamic range (and such good phase stability) as observers imaging bright emission complexes. The loss of point source response produced by poor phase stability in a detection experiment can be estimated by calibrating with a long (e.g., > 2 hour) interpolation of the gains, then imaging the calibrators and comparing their apparent flux densities in these images with their assumed values.

b) Self-calibration.

The most reliable method for removing atmospheric fluctuations from the data is self-calibration, *if the target is strong enough.* Self-calibration should be used if the signal-to-noise on the target is high enough to determine the gains in the typical coherence time $\tau_{\rm atm}$ of the atmospheric phase screen, using baselines involving all antennas. For an array of N elements, the r.m.s. noise in the determination of an individual antenna phase gain by self-calibration on a point source of flux density $S_{\rm sc}$ Jy will be

$$\phi_{\rm rms} \approx \frac{65\Delta S}{S_{\rm sc}\sqrt{(N-2)\Delta\nu\tau_{\rm sc}}} \text{ degrees}, \qquad (24\text{–}4)$$

where ΔS is the sensitivity in Jy per second per MHz of bandwidth, and $\tau_{\rm sc}$ is the averaging time used for the gain solutions. Unless $\phi_{\rm rms} \ll 60°$ when $\tau_{\rm sc} = \tau_{\rm atm}$, self-calibration will not improve the data.

There are several reasons why external calibration is useful even if you know you will be able to self-calibrate your final images. External calibrators will provide flux-density and position scales for self-calibrated images (on which this information will otherwise generally be lost). Observations of the time scale of the phase fluctuations on a phase calibrator near your target can also be used to estimate the coherence time $\tau_{\rm atm}$ of the atmosphere during your observations. This will enable you to select a suitable averaging time $\tau_{\rm sc}$ for the self-calibration: it should be $\leq \tau_{\rm atm}$. Such observations may also tell you that some parts of your data were obtained under more stable atmospheric conditions than others; the "good" parts may yield a better initial model of your target that helps self-calibration of the whole data set to converge quickly.

Fortunately, the class of source for which images of high dynamic range are most important is also the class for which self-calibration is most likely to

work well—namely, those with weak extended structures around bright small-diameter components, as discussed in Lecture 16. There is however a range of flux densities and structural complexities over which self-calibration cannot be guaranteed to work in typical atmospheric coherence times $\tau_{\rm atm}$, and for which external calibration therefore remains essential.

7.3. Position calibration.

The phase referencing that is done during external calibration refers the absolute position scale of the images to the mean position scale defined by the adopted positions of the external phase calibrators, if the antenna co-ordinates are well determined. No further positional calibration is required for routine (non-astrometric) synthesis imaging. Note however that *self-calibration* fundamentally has no absolute phase reference and therefore produces images whose position scale is whatever was specified in the input model.

7.4. Flux density calibration.

The flux density scale is usually set by observing an unresolved reference source whose flux density is believed to be stable and whose intensity has previously been measured on an absolute scale. As there are few such sources that remain unresolved to long-baseline arrays, it is rarely possible to use a primary flux density calibrator also as the primary phase calibrator. Good phase calibrators are strong and unresolved, so are likely to vary with time. The flux densities of phase calibrators must usually be determined at the time of the observations by measuring their amplitude ratios to standard flux density calibrators, often using only a short-baseline subset of all the antennas in the array. Note that self-calibration has no absolute amplitude scale and therefore produces images whose flux density scale is whatever was specified in the input model.

7.5. Polarization calibration.

The quantities to be calibrated are the individual antenna cross-polarization terms and the position angle scale (including any time-variable ionospheric Faraday rotation). The design of this calibration depends on whether the antennas are on equatorial or altitude–azimuth mounts, and on the feed polarizations. The VLA case is described in the Appendix.

7.6. Bandpass calibration.

Spectral line observers must also calibrate the instrumental bandpass, often for both amplitude and phase. The amplitude calibration may sometimes be estimated by dividing the cross-correlation spectra by the geometric mean of the autocorrelation spectra of the relevant antennas. This approach is unsuitable however if there are lines (or interfering signals) in the passband that are strong enough to show up in the single-antenna spectra. It is inadequate if the phase variation across the band is significant relative to other uncertainties, for example those imposed by the signal-to-noise ratio.

The most complete approach to bandpass calibration is to observe a strong line-free continuum source to find the bandpass characteristics (amplitude and phase) of each antenna-receiver combination. In a well-engineered system, these characteristics will be only slow functions of time, so the calibration need not

be repeated often. Notice however that the total time needed for the bandpass calibration is set by the sensitivity required to measure the gain *in each channel* as accurately as needed for the required *spectral* dynamic range. Projects that require high spectral dynamic range may therefore have to invest a large fraction of the total observing time in bandpass calibration. See Lecture 18 for details of bandpass calibration strategy.

8. Stormy Weather and What to Do About It

Some observing programs have frequency agility. For these, it may be practical to adjust the strategy to take account of the weather during the observing run. But note that "you can't tell the phase stability by looking out of the window"[4]—you must *observe* to find out how stable the phases are. It is difficult either to predict phase stability in advance (except to say that it is likely to be bad because a storm front is passing, for example) or to judge it during the observations by "looking out of the window". Clear blue skies do not guarantee stable phases. Thunderstorms do however guarantee unstable phases!

If your program has frequency agility, it is a good idea to monitor the phase of a strong calibrator for a few minutes on a long baseline as you start observing. Fluctuations of order a radian on a time scale of minutes are unmitigated bad news, and the only possible strategy is to move the observations to lower frequencies if this makes astronomical sense. The converse is not true, however. Short-term (minute-by-minute) phase stability to within a few degrees does not guarantee that the observations will be of good quality for synthesis. Synthesis imaging requires stability over the time scale of your calibration cycle (unless you are going to self-calibrate). You should therefore pay attention to the phase changes between *adjacent* scans of your calibrator, as well as to that within the scans, to assess whether you have the stability needed for synthesis. If the longer-term stability is marginal, i.e., of order 30°–40° between calibrations, you might consider using a faster calibration cycle.

Acknowledgments

I thank Ron Ekers, Rick Perley, Fred Schwab, Jacqueline van Gorkom, Arnold Rots, and many students who attended the 1982 and 1985 NRAO Summer Schools in Socorro, for valuable comments on earlier versions of this lecture.

[4] Words of wisdom widely promulgated during the early days of the VLA, and attributed to Barry Clark.

Appendix A: Considerations Specific to the VLA

To avoid burdening the main text with VLA-specific details that may obstruct the view of the lecture's general principles, I have collected as many of these details as possible into this Appendix. Readers who are interested in using other radio synthesis arrays may also find this Appendix helpful as a "worked example" of points discussed earlier.

A1. Choosing a VLA Configuration

a) Standard configurations.

An image made from untapered uniformly-weighted ≥ 4 hour tracks in a standard VLA configuration when foreshortening of the array is unimportant has a synthesized beam B with a half-power beamwidth given approximately by

$$\theta_{\rm HPBW} = 1\farcs25 \times \frac{1480}{\nu_0} \times 3.285^{n-1}\,, \qquad (24\text{–A1})$$

where ν_0 is the observing frequency in MHz and $n = 1$, 2, 3, or 4 for the **A**, **B**, **C**, or **D** configuration, respectively.

It is most important to choose a suitable combination of ν_0 and n when planning VLA observations. For example, consider a smooth two-dimensional emission region 30″ across with a peak apparent brightness $I\Omega_s$ of 1 mJy per beam area on an untapered 20 cm image made with the VLA **B** configuration (resolution $\approx 4\farcs2$). The same region will have a peak apparent brightness of only 0.093 mJy per beam area on an untapered 20 cm image made with the same hour-angle coverage and u-v weighting in the **A** configuration (resolution $\approx 1\farcs3$). It could be detected at the 10σ level in about 16 min of integration at 50 MHz bandwidth in the **B** configuration (using the sensitivity data given in Table 24–2), but a 10σ detection in the **A** configuration using the same bandwidth would require about 31 hours of on-source integration! It is is therefore *extremely* important not to use a VLA configuration that gives a smaller beam area Ω_s than is strictly necessary, when studying extended emission.

Note also that the effects of spectral index and resolution combine to make extended *steep-spectrum* emission much harder to detect with a given VLA configuration at the higher frequencies. For example, suppose that an extended emission region has a peak intensity of 1 mJy per 'CLEAN' beam area in the VLA's **A** configuration at 20 cm—a 10σ detection would be made in 16 minutes at 20 cm. If the region has a ν^{-1} spectrum, the peak intensity in the **A** configuration at 6 cm would be 0.027 mJy per 'CLEAN' beam area and a 10σ detection at this frequency would require 160 hours of integration. The choice of observing frequency is therefore critical when trying to detect steep-spectrum extended emission using a given VLA configuration.

For sources with compact flat-spectrum components *and* extended steep-spectrum emission, the dynamic range needed to image the extended structure increases rapidly with increasing frequency. Suppose that the extended emission referred to in the previous example surrounded a 5 mJy point source with a ν^0 spectrum. The dynamic range required for 10σ detection of the extended structure would be 50 : 1 in the **A** configuration at 20 cm. This is easy to obtain. The dynamic range required in the **A** configuration at 6 cm would be 1850 : 1, a non-trivial goal without self-calibration.

b) Combinations of standard configurations.

Options other than the standard (**A, B, C, D**) configurations of the VLA are available. You will need to combine observations made in more than one VLA configuration if you require a *range* of baselines that exceeds the range provided by a standard configuration.

As the ratio of the longest to the shortest baseline in a standard configuration of the VLA is about 40 : 1, each standard configuration can be used to image reliably up to $\theta_{\rm LAS} \approx 40\theta_{\rm HPBW}$ where $\theta_{\rm HPBW}$ is given by Equation 24–A1 at the specified frequency. If the values of $\theta_{\rm LAS}$ and $\theta_{\rm HPBW}$ needed for your experiment do not *both* fall between $\theta_{\rm HPBW}$ and $40\theta_{\rm HPBW}$ calculated from Equation 24–A1 for a given standard configuration and frequency, consider using more than one VLA configuration—unless you can extend the projected baseline range by

observing at extreme hour-angles (where the u-v baselines may be significantly foreshortened). Observations requiring $\theta_{\rm LAS}/\theta_{\rm HPBW} > 40:1$ generally require more than one configuration, but some with $\theta_{\rm LAS}/\theta_{\rm HPBW} < 40:1$ have the same need—for example, if the optimum $\theta_{\rm HPBW}$ falls mid-way between two resolutions given by allowed values of n and ν_0 in Equation 24–A1.

For example, Figure 24–3 shows the u-v coverage of the VLA at +60° declination for 12 hours observing in the **A** configuration, and for 6 hours of **A** configuration observing combined with 6 hours in the **C** configuration. The "hole" at the center of the u-v coverage in Figure 24–3 could be filled by mixing data from the **A** and more compact configurations. Consider mixing standard-configuration observations for any source for which $\theta_{\rm LAS}/\theta_{\rm HPBW}$ is significantly greater than 40 : 1. The total integration times needed in the different configurations should be computed separately; most projects will not need as long a total integration time in the more compact configurations as in the more scattered ones.

c) Hybrid configurations.

"Hybrid" configurations are available during reconfigurations, when the arms of the VLA may either be of different length, or have a non-standard assortment of long and short baselines. Some hybrid configurations provide wider ranges of u-v spacing than can a standard configuration (giving sensitivity to a wider range of angular scales). Some can help self-calibration of data from a compact configuration by providing unusually long spacings.

Hybrid configurations with long North arms are now regularly scheduled at the VLA. They are useful when imaging regions south of $\delta \approx -15°$, where the north–south extent of the u-v coverage of the standard configurations is seriously foreshortened by projection. Figure 24–4 shows the u-v coverage for the **B** configuration at $\delta = -40°$, compared with that of a hybrid configuration whose East and West arms are in the **B** configuration but whose North arm is in the **A** configuration. The spacings involving the longer North arm fill in a region around the v-axis that is left empty by the standard **B** configuration. This **A/B** hybrid is available briefly about every sixteen months, during a reconfiguration from **A** to **B**. Similar **B/C** and **C/D** hybrids are scheduled between the appropriate reconfigurations.

Perley (1981b) examined whether other hybrid VLA configurations could usefully extend the ratio of maximum to minimum baselines in synoptic observations with the VLA. In general, you get better u-v coverage by mixing data from two different standard configurations than by spending the same total time in *any* hybrid configuration. No other hybrid VLA configurations are regularly scheduled.

d) Sub-arrays.

"Sub-arrays" are nonstandard configurations obtained by dividing the VLA into smaller arrays that are devoted to different observing programs at the same time. The use of sub-arrays is generally not as efficient as time-sharing the entire VLA. The number of interferometer pairs in a sub-array is $N(N-1)/2$ where N is the number of antennas in the sub-array. Sub-arrays with 13 and 14 antennas therefore have 78 and 91 interferometers respectively, whereas a 27-antenna standard configuration has 351. An hour of observing in which two such sub-arrays each perform different tasks therefore produces 169 interferometer-hours of data. In contrast, two half-hours of observing, with the full VLA devoted to each task in turn, produce 351 interferometer-hours of data. Dedicating two roughly equal sub-arrays to different tasks thus reduces the amount of information gathered by a factor of about two, compared with time-sharing the whole VLA between the two tasks. This loss of information manifests itself as poorer sensitivity and u-v sampling in the sub-array data. The use of sub-arrays is therefore generally undesirable unless you need *strictly* simultaneous observations of strong sources at several frequencies (e.g., to measure instantaneous spectra of rapid variables) or to study many compact sources quickly with only modest demands on sensitivity and dynamic range (e.g., for astrometry of strong sources).

e) "Scaled" configurations.

Returning to Equation 24–A1, note that the scaling factor between "adjacent" VLA configurations (e.g., **B** and **C**) is 3.285. This factor is close to the ratios between the default VLA frequencies at 20 cm and 6 cm and between those at 6 cm and 2 cm. The VLA therefore

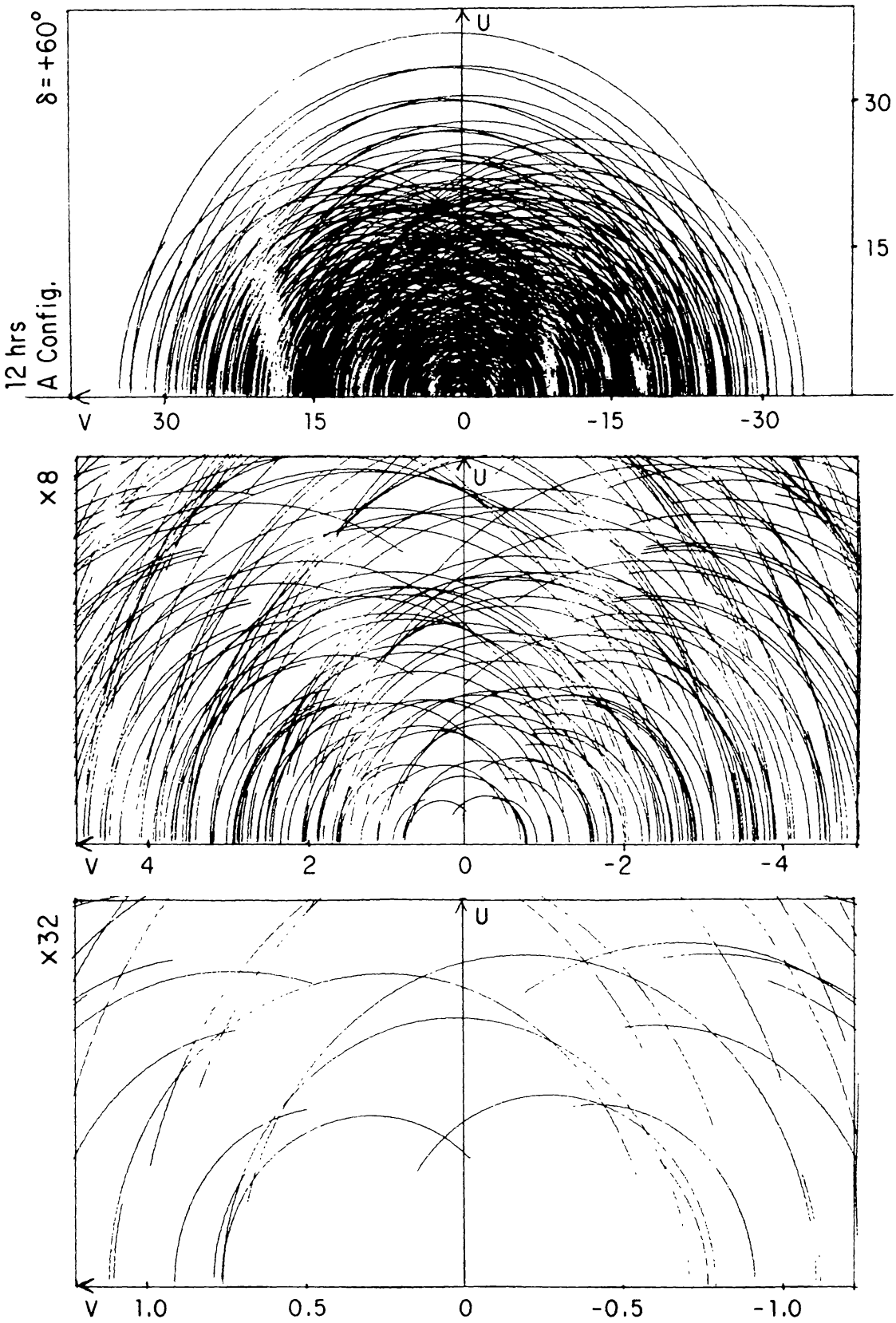

Figure 24–3. u-v coverage for $\delta = +60°$ in the **A** configuration (12-hour tracks).

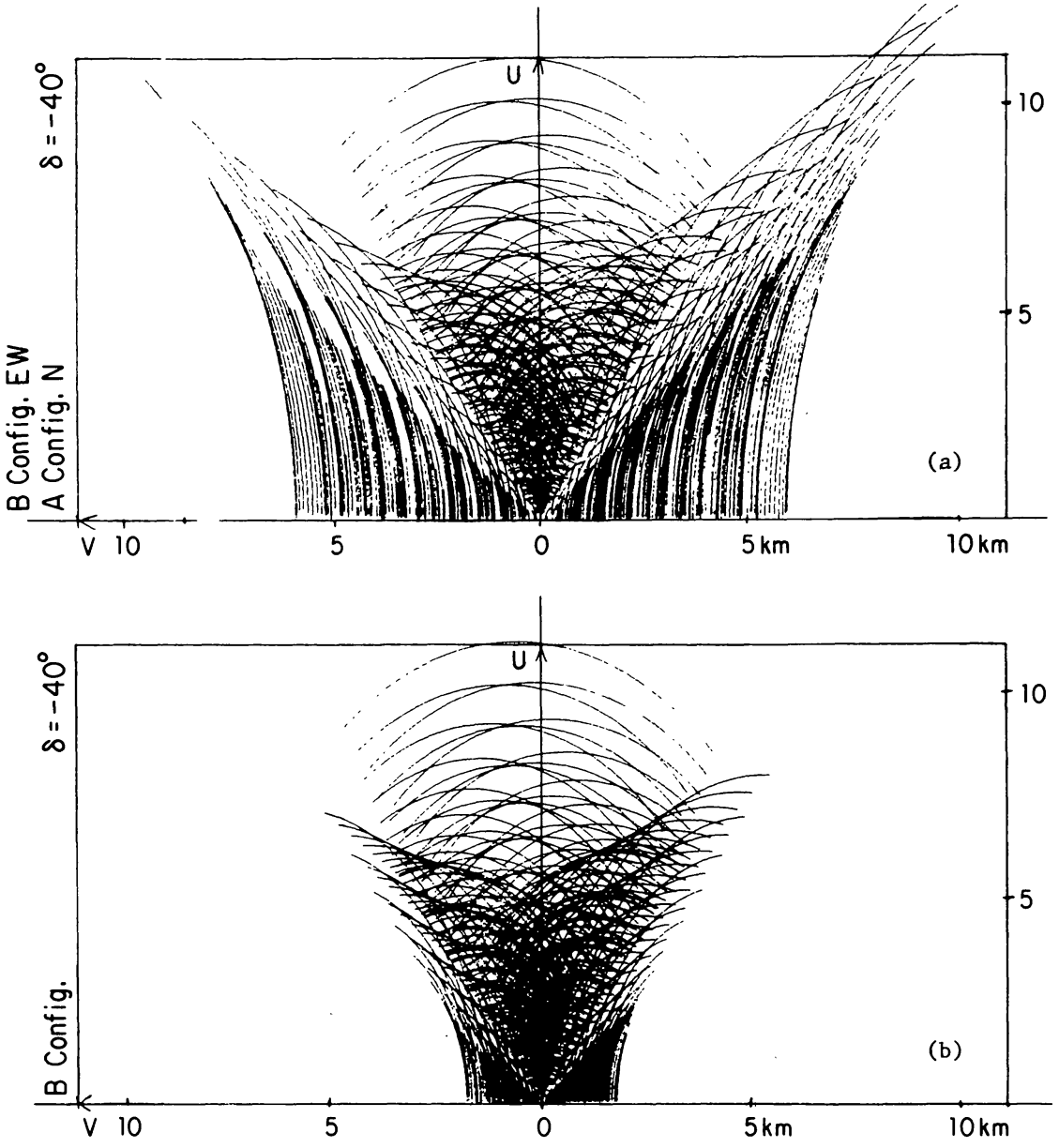

Figure 24–4. *u-v* coverage at $\delta = -40°$ with **(a)** the VLA East and West arms in **B** configuration and the North arm in **A** configuration, and **(b)** the entire VLA in **B** configuration.

has similar resolutions at 20 cm in the **A** configuration, at 6 cm in the **B** configuration, and at 2 cm in the **C** configuration. (Such rough three-frequency scalings also apply for the **B**, **C**, and **D** configurations, of course.) These scalings make the VLA a powerful tool for studies of the frequency-dependence of the properties of extended emission.

A2. Frequency Selection

Table 24–1 lists the frequency bands now available at the VLA.

Table 24–1.
VLA Observing Frequencies

Frequency Range	Band Name	System Temperature	Antenna Efficiency
0.3 to 0.35 GHz	P Band (90 cm)	125	0.40
1.26 to 1.73 GHz	L Band (20 cm)	60	0.51
4.5 to 5.0 GHz	C Band (6 cm)	50	0.65
8.0 to 8.8 GHz	X Band (3.6 cm)	30	0.58
14.4 to 15.4 GHz	U Band (2 cm)	116	0.52
22.0 to 24.0 GHz	K Band (1.3 cm)	150	0.43

The VLA continuum system lets you observe at two independent sky frequencies within each "band". This capability can be used to increase sensitivity, to fill in the u-v plane more densely by crude "bandwidth synthesis" (see Lecture 12, Section 1.1) or to study spectral or Faraday depth changes in your source across a "band" (the latter being especially worthwhile across the 'L' Band).

Interference is rarely detected or suspected above 1.8 GHz at the VLA. It is an important factor in choosing a continuum observing frequency within the L Band (1260 to 1730 MHz), particularly when using non-standard frequencies (e.g., when seeking to observe at the opposite edges of the band to determine Faraday rotation parameters). As spectral line observers do not have freedom to choose center frequencies for their projects, L Band interference may determine whether a given spectral line experiment is possible. There is self-generated interference throughout L Band at the VLA, mainly at the harmonics of 50 MHz; this internal interference should be below the noise in any continuum image made with an IF bandwidth $\Delta\nu > 6.25$ MHz, but can be a serious problem for spectroscopy.

Before using a non-standard frequency below 2 GHz, consult with VLA scientific staff (particularly Pat Crane, the VLA frequency coordinator) for advice and lore based on recent observers' experiences.

A3. Bandwidth

Users of extremely narrow bandwidths should be aware that when observing in continuum mode the VLA bandwidths narrower than 6.25 MHz suffer large closure errors because the quadrature networks do not work well. If such narrow bandwidths are essential for your observations, consider observing with the spectral-line system, where these problems are avoided. The VLA spectral-line system is not a panacea for eliminating chromatic aberration, however. It cannot (yet) support continuum polarimetry fully (and—because of the need to supply 'channel 0' for spectroscopy—it will not provide more than 3 "IFs" at 50 MHz total bandwidth even when completed in late 1989).

Chromatic aberration effects at the VLA are well estimated by the expressions given in Lecture 13 for a square bandpass and Gaussian tapering in the u-v plane. In the regime $(0 < \beta \leq 1)$ where the amplitude reduction for a point source is moderate, the exact expression for the reduction (Lecture 13, Equation 13–23) can be approximated by

$$\frac{I}{I_0} \approx 1 - \frac{1}{3}\left(\frac{\gamma\Delta\nu\theta}{2\nu_0\theta_{\rm HPBW}}\right)^2 + \frac{1}{10}\left(\frac{\gamma\Delta\nu\theta}{2\nu_0\theta_{\rm HPBW}}\right)^4, \qquad (24\text{–A2})$$

using the standard expansion for the error function, erf, at small values of its argument.

A4. AVERAGING TIME

The on-line visibility averaging time τ_a at the VLA may be set to any multiple of $1\frac{2}{3}$ sec, but the even multiples are preferable, for reasons associated with the VLA phase switching system. In practice, averaging for only 1.67 sec may give large ($\sim$ 10 mJy) correlator offsets, so the shortest τ_a recommended for all applications is 3.3 sec. The "default" values of the on-line visibility averaging time τ_a at the VLA are 10 sec for the **A** and **B** configurations and 30 sec for the **C** and **D** configurations.

The effects of the on-line averaging are permanent, because the averaged data are written to the archive tape created by the on-line system. It is therefore important to choose an on-line averaging time that limits time-averaging distortions to acceptable values, and is shorter than the expected atmospheric coherence time (provided the hardware and computer restrictions permit such a choice—spectroscopists must note Table 24–6). Longer averaging times may be used off-line, e.g., once the data have been calibrated.

For Gaussian tapering in the u-v plane, the intensity reduction due to a finite averaging time τ_a is given by Equation 13–39 with $\alpha = \gamma^2/\pi^2$, which we may write as

$$\frac{I}{I_0} \approx 1 - \frac{\gamma^2}{12}\omega_e^2\tau_a^2\left(\frac{\theta}{\theta_{\rm HPBW}}\right)^2 . \qquad (24\text{–A3})$$

Spectroscopists should use Equation 24–A3, with values of I/I_0 that are acceptable for their experiment, to determine the maximum acceptable averaging time.

Continuum observers may wish instead to use an averaging time $\tau_{\Delta\nu}$ that produces the *same* intensity reduction for a source near the pole as does an IF bandwidth $\Delta\nu$. This can be approximated (for small intensity reductions) by equating the terms in $\theta^2/\theta^2_{\rm HPBW}$ from Equations 24–A2 and 24–A3, obtaining

$$\tau_{\Delta\nu} \approx \frac{\Delta\nu}{\omega_e\nu_0} = 1.375 \times 10^4 \frac{\Delta\nu}{\nu_0} \text{ sec} . \qquad (24\text{–A4})$$

Equation 24–A4 gives a reasonable criterion for the maximum averaging time τ_a that should be used with an IF bandwidth $\Delta\nu$ for continuum observations at observing frequency ν_0.[5] Notice that $\tau_{\Delta\nu}$ does not depend on VLA configuration or on $\theta_{\rm max}$, owing to the first-order similarities between the bandwidth and time-average smearing for a polar source. Lecture 2 gave an intuitive basis for Equation 24–A4: for a polar source, time averaging smears the visibilities over an *angle* $\omega_e\tau_a$ in the u-v plane so its effects scale as $\sqrt{l^2+m^2}\,(\omega_e\tau_a)$, whereas those of bandwidth smearing scale as $\sqrt{l^2+m^2}\,(\Delta\nu/\nu_0)$.

You may have to exceed the value of $\tau_{\Delta\nu}$ calculated from Equations 24–A3 or 24–A4 because the VLA's on-line system cannot provide averaging times less than 1.67 seconds in any of the normal observing modes. Note also that the VLA on-line system averages all baselines with the same τ_a, and that the 'FILLER' program used to convey data to the DEC-10 off-line system imposes the *same* averaging time for the target and calibrator observations.[6] If the calibrator observations are only a few minutes each (as is often the case at low frequencies), averaging times longer than 1 min are undesirable because they permit only crude editing of the calibrator data. τ_a is also limited in many cases by the size of the final data set, especially for multiconfiguration continuum syntheses, or multichannel—continuum or spectral line—observing (Table 24–6). If storing the data set requires much more than the average disk space available per user in the off-line computers, data processing (and/or life with one's colleagues) becomes difficult. Averaging times τ_a are sometimes set longer than would otherwise be desirable, just to avoid "excessive" data volumes. Remember that one 512-byte "block" of disk in most computers that run AIPS stores 7.53 VLA visibility records, so a VLA continuum data set with both the AC and BD IFs uses about $93t_{\rm int}/\tau_a$ such disk blocks.

[5] It differs slightly from the formula in earlier versions of this lecture, due to my use here of more accurate expressions for the smearing effects from Lecture 13.

[6] This restriction has been removed in the 15OCT88 release of the corresponding AIPS task, 'FILLM'.

Most VLA continuum observing is done with 10 sec $< \tau_a <$ 1 min because of these constraints. For line work, the minimum averaging time and the number of spectral line channels are linked by computer usage rules at the VLA, but observers who will process their data away from the VLA may exceed these limits (if they can accommodate the resulting data sets at home!). Table 24–6 gives the rules that are in force in late 1988. Confirm them when planning a spectral line proposal—the details change with time, and changes are published in the *NRAO Newsletter* and the *VLA Observational Status Report.*

A5. THE PRIMARY BEAM

To first order, the primary beam of the VLA antennas can be taken to be a Gaussian with FWHM equal to $90\lambda_{cm}$ arcsec, and this approximation suffices for most proposal planning. In standard VLA software, the primary beam correction ($1/\mathcal{A}$, Lecture 3) is modeled by a power law expansion of the form $\frac{1}{\mathcal{A}} = \sum a_i X^{2i}$ where $X = \theta_{arcmin}\nu_{GHz}$ and the coefficients are $a_0 = 9.920378 \times 10^{-1}$, $a_1 = 9.956885 \times 10^{-4}$, $a_2 = 3.814573 \times 10^{-6}$, $a_3 = -5.311695 \times 10^{-10}$, and $a_4 = 3.9809630 \times 10^{-12}$ (Napier and Rots 1982). This correction is usually not applied at small values of X for which the Napier–Rots expansion gives $\mathcal{A} > 1$. It is not well determined at large values of X for which $\mathcal{A} < 0.15$.

A6. SENSITIVITY

Table 24–2 gives the theoretical r.m.s. noise on I and P images made at the VLA without tapering, using 27 antennas and the maximum interference-free continuum bandwidths, for integration times typical of "snapshots" (see below) and of more complete syntheses.[7] (Interference normally restricts observations at 92 cm to a 3 MHz bandwidth.)

Table 24–2.
Theoretical R.m.s. Noise on Images Made with 27 VLA Antennas*

Band Designation:	92 cm P	20 cm L	6 cm C	3.6 cm X	2 cm U	1.3 cm** K
ΔS (1 sec, 1 MHz), Jy	1.87	0.60	0.45	0.31	1.14	2.40
Bandwidth $\Delta\nu$, MHz	3	50	50	50	50	50
R.m.s. noise in 5-min "snapshot", mJy/beam	2.4	0.19	0.15	0.10	0.37	0.78
R.m.s. noise in 12-hr integration, mJy/beam	0.20	0.016	0.012	0.008	0.030	0.064

*For two IFs and natural weighting. For uniform weighting, multiply all entries by 1.5 (for a first approximation).
**1.3 cm values are for the new (1988) receivers.

A7. "SNAPSHOT" MODE

The "Y" layout of the VLA produces an *instantaneous* synthesized beam with a respectable shape and sidelobe level. It is therefore possible to do interesting science with brief observations if the targets are both bright and compact. Snapshot mode observing may be ideal for observers who wish to study statistical properties of large samples of sources (and also to overdose on synthesis image processing!).

In what follows, I consider a single "snapshot" to be an observation of $<$ 5 minutes' duration. Snapshots of $<$ 1 minute duration may even be appropriate if you want to image many ($>$ 1000) fields that are near to one another on the sky (so that antenna drive times are also short) and it does not matter if the occasional observation is abbreviated or even lost.

[7] Note that some system parameters (e.g., sensitivities) that affect these decisions will improve with time as a result of hardware upgrades, etc. NRAO publishes a *VLA Observational Status Report* that summarizes relevant system parameters at least once per year. You should check the most recent copy of this *Report* when planning a VLA proposal.

a) Limitations of "snapshot" mode.

The clearest limitation of snapshot observing is sensitivity (see Table 24–2); snapshot mode is suitable only for bright sources. Below 2 GHz, the high sidelobe levels of snapshot beams exacerbate the problems created by confusing sources, and snapshots of fields near the galactic plane using the more compact VLA configurations are frequently dominated by sidelobe clutter from confusing sources rather than by the noise that is quantified in Table 24–2. These problems are less severe above 2 GHz because of the smaller primary beam and the typical source spectrum (see Section A9 on "Confusion" below).

The second limitation of snapshot observing is the restricted angular size scale $\theta_{\rm LAS}$ over which the u-v coverage of a snapshot (e.g., Fig. 24–5) satisfies the sampling theorem and thus permits reconstruction of the correct sky brightness distribution. Table 24–3 estimates this limitation for snapshots on the meridian in the standard VLA configurations and frequencies, averaged over all declinations.

Table 24–3.
Approximate Values of $\theta_{\rm LAS}$ for a Single Snapshot*

	A	B	C	D
92 cm	140″	8′	23′	50′
20 cm	30″	100″	5′	12′
6 cm	9″	30″	90″	200″
3.6 cm	6″	18″	53″	120″
2 cm	3″	10″	30″	70″
1.3 cm	2″	7″	20″	45″

*Larger structures can be imaged by combining a few snapshots taken at different hour angles.

Polarization calibration may be difficult for short snapshot programs; it is not easy to verify the instrumental polarization calibration for a program whose total observing time is only a few hours, as this calibration requires at least three observations of a calibrator spanning a change in parallactic angle χ of $\Delta\chi \geq 90°$ (see Lecture 5, Section 7.1). "Standard" instrumental polarization parameters may then have to be used—note that these are available only for a few "standard" combinations of VLA observing frequencies and bandwidths (the default frequencies for 50 MHz bandwidths at 20 cm, 6 cm and 2 cm, and the default frequencies for 25 MHz and 12.5 MHz bandwidths at 6 cm). Position angle calibration may also be difficult if the standard polarization calibrators are not readily observable during the time allocated to a snapshot program. Snapshooters interested in polarimetry should ensure that suitable polarization calibration is possible when designing their program, by giving attention to its LST range and the choice of observing frequencies and bandwidths.

Snapshots are most effective when all sources are observed within about 2 hours of the meridian. At larger hour-angles, foreshortening of the array leads to poorer sampling of the u-v plane, elliptical synthesized beams, etc.

The time taken to calibrate a snapshot data set is determined mainly by the total observing time. Snapshot programs require the same calibration effort as simple synthesis programs of the same total duration. The image construction, deconvolution and display steps of snapshot observing can require large amounts of computer time and your time, however. As a snapshot image of a given target may be as large as a full synthesis image of the same field, snapshot programs also make heavy demands on disk storage. This can be especially true for snapshots made in the more compact configurations below 2 GHz, which are particularly prone to degradation by sidelobe clutter from confusing sources. Snapshooters must therefore be prepared to coordinate their data reduction requirements with those of other users, and to adopt efficient reduction strategies, including backing up of inactive images, beams and u-v data sets whenever possible.

b) Multiple snapshots versus extended snapshots.

Snapshots require phase stability only for the duration of the individual snapshot. There is therefore some debate over whether (for example) an observation requiring 15 minutes of

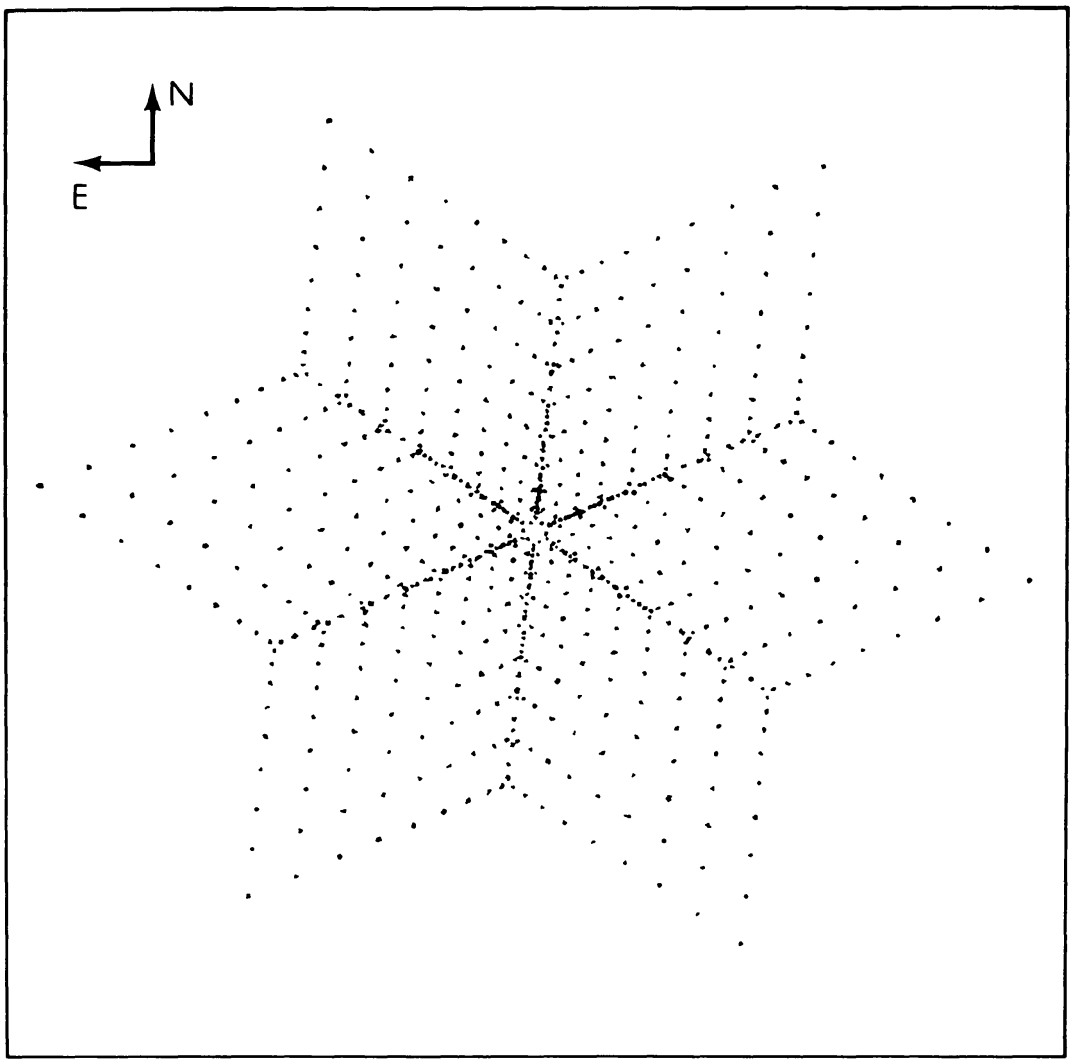

Figure 24–5. The u-v plane coverage for an instantaneous sampling of data for a source at $\delta = 30°$ and $H = 0$ by the 27-antenna VLA.

integration time $t_{\rm int}$ is better made as one continuous 15-minute observation or by combining the data from three separate 5-minute snapshots. A single 15-minute observation may give better dynamic range, because ionospheric or tropospheric phase gradients in the form of "wedges" may calibrate out of a single short observation, leaving only a position shift. In contrast, three shorter observations that are more dispersed in time and calibrated on a long calibrator cycle may encounter different wedges and so combine to give an image with poorer final dynamic range, unless self-calibration (Lecture 9) can be used. There are therefore some circumstances in which a single observation is preferable, as well as being easier to schedule.

The advantages of combining data from several shorter snapshots are (a) greater protection against total loss of the data for a given source through equipment failures or short-term bad weather, and (b) more even sampling of the u-v plane than in a single extended snapshot. Multiple snapshots are particularly useful when observing at wavelengths of 18 cm and longer in the **C** and **D** configurations, as they allow better imaging of confusing sources that may otherwise limit the achieved dynamic range (see Section 6 below). The single extended snapshot may be better for observations that must be made at low elevations, where phase "wedges" are more likely to arise, and if self-calibration cannot be used. This may be particularly true for observations of weak or complex low-declination sources for which the total hour-angle

coverage is anyway limited by the short time that a given source is above the horizon.

A8. Spectral Line Observing

The VLA correlator has enough chips to produce 16 complex frequency channels at the nominal "50 MHz" (46 MHz) bandwidth. Halving the total bandwidth allows the chips to be "time-shared" so that the number of channels is doubled. This total bandwidth halving and time-sharing can be continued to a maximum of 512 channels, at which point further halvings of the total bandwidth leave the number of channels at a maximum of 512. Table 24–4 summarizes the resulting channel number and channel width options for a single IF, with and without on-line Hanning smoothing. Hanning smoothing to reduce the Gibbs phenomenon is strongly recommended for all observations that require high spectral dynamic range; it may be applied either on-line or off-line.

Table 24–4.
Total Channels in VLA Spectral Line Modes

Bandwidth (MHz)	Without Hanning Channels	Without Hanning Separation (kHz)	With Hanning Channels	With Hanning Separation (kHz)
0.195313	512	0.381	256	0.763
0.78125	512	1.526	256	3.052
1.5625	512	3.052	256	6.104
3.125	256	12.207	128	24.414
6.25	128	48.828	64	97.656
12.5	64	195.313	32	390.625
25	32	781.25	16	1562.5
46	16	3125	8	6250

The above total numbers of channels may also be split evenly among two, or four, IFs. For example, if an observation is set up at 12.5 MHz total bandwidth with 2 IFs and no on-line Hanning smoothing, there will be 32 channels in each of the two spectra (i.e., 32 per spectrum for a total of 64 as shown in the table). The splitting among the IF channels is selected on the //DS input "card" by specifying the correlator "mode". Note that the first channel ("channel 0") of each IF contains the complex average of the central 75% of the band that the correlator has available (even if not all of that band has been selected).

The on-line system update of August 2, 1988 made available three new spectral line modes that support two IFs—modes 2AC, 2AD and 2CD. Other modes are planned that will use the entire correlator (including full polarization) but are not supported yet. All old modes (2A, 2C, 2D, 4A, 4D) that use only a fraction of the correlator are still supported at the time of writing this lecture, but will be phased out once all the new modes are in place—probably in the last quarter of 1989. Table 24–5 shows the VLA spectral line correlator modes that will be supported once the on-line system is fully upgraded, under the following headings:

Mode: Correlator Mode as expressed on the //DS input "card".

Supported?: "Yes", if it is available in the current (late 1988) system; "No" if it is not likely to be available until late 1989.

Number of IFs: The number and VLA designation of the IFs recorded on the archive tape.

For further details of correlator options and strategy decisions that involve them, read Rots (1988) or Sowinski and Braun (1988).

Table 24–6 gives the current averaging time restrictions that are imposed at the VLA to limit the burden on the off-line data reduction systems. These restrictions do not apply to data sets that will be reduced entirely outside the VLA off-line computers. These rules may change with time, and VLA staff and the *NRAO Newsletter* should be consulted for updates.

Table 24–5.
VLA Spectral Line Correlator Modes

Mode	Supported?	Number of IFs
1A	Yes	1 A
1B	Yes	1 B
1C	Yes	1 C
1D	Yes	1 D
2AB	No	2 A,B
2AC	Yes	2 A,C
2AD	Yes	2 A,D
2BC	No	2 B,C
2BD	No	2 B,D
2CD	Yes	2 C,D
4	No	4 A,B,C,D
4PA	No	4 A,C
4PB	No	4 B,D

Table 24–6.
VLA Averaging Time Restrictions

Channels	Minimum (sec)
1	3.3
8	5
16	7
32	15
64	60
128	120
256	240
512	480

A9. CONFUSION

The number of extragalactic sources N per square arc minute of sky with flux densities greater than S mJy at 6 cm can be written approximately as

$$N(>S) = 0.032S^{-1.13} \tag{24–A5}$$

over the flux density range that is relevant for confusion calculations at the VLA (e.g., Ledden *et al.* 1980). The corresponding expression at 20 cm is

$$N(>S) = 0.10S^{-0.9}\,. \tag{24–A6}$$

The analogs of these expressions for 2 cm and 1.3 cm are not known directly from measured source counts. They could be *estimated* from the 6 cm count in Equation 24–A5 by scaling flux densities to 6 cm with an effective mean spectrum of $\sim \nu^{-0.6}$.

Images made at 20 cm will contain, on average, one extragalactic source of flux density 110 mJy closer to the field center than the 15′ HWHM of the primary beam. The 6 cm primary beam (4.′5 HWHM) will contain, on average, one extragalactic source of flux density 2 mJy, the 2 cm beam (1.′85 HWHM) a source of < 0.1 mJy and the 1.3 cm beam (1′ HWHM) a source of < 0.01 mJy. At 92 cm, there is always at least one several-Jy source in the primary beam and there may be many. Individual pathological cases aside, confusion is unlikely to be a problem at wavelengths shorter than 6 cm. At 20 cm and 6 cm it may be a problem in the VLA's more compact configurations. At 92 cm it is a problem in *all* configurations.

Confusion is particularly troublesome for snapshooters using the compact configurations below 2 GHz, because the sidelobes resulting from the "snowflake" u-v coverage of snapshots

(Fig. 24–8) are extensive. Images at low galactic latitudes are also more confused than those at high galactic latitudes. Snapshooters should plan to reduce their data using the ungridded subtraction algorithm ('MX' in AIPS) both because it permits imaging of multiple subfields and because it eliminates the effects of sidelobe aliasing.

A10. Calibration Details

a) Instrumental and atmospheric monitoring.

Reference sources should generally be chosen from the *VLA Calibrator List* maintained at the site by the NRAO staff, unless you are sure that a putative calibrator is unresolved in the VLA configuration that will be used, and has a position measured in the VLA reference system to better than 0.1 arcsec.

The length of time spent on each calibration scan should be enough to achieve a signal-to-noise (over the 26 baselines contributing to each antenna gain solution) commensurate with the required calibration accuracy. Never plan to calibrate for less than 1 minute at a time, however, as shorter calibrator scans may be lost as a result of unusually long settle-down times, etc. Significant atmospheric amplitude and phase fluctuations can occur on time scales of minutes, even at wavelengths of 6 cm and longer. When the Sun is active, *ionospheric* fluctuations will dominate at 18 cm and longer—they can also be rapid on long VLA baselines. It is completely impractical to adopt a *calibrator/target/calibrator* cycle that will guarantee following the fastest fluctuations of either kind. Keep in mind that *no* external referencing, no matter how rapid, can be *guaranteed* to remove atmospheric fluctuations from the data, and that time spent driving to and observing calibrators is time deleted from integration, and u-v coverage, on your target. You must decide for yourself how to play this particular roulette game during a given run.

Typical VLA observing programs spend from 5% to 10% of their time on calibration at the lower frequencies; more calibration may be needed at the higher frequencies where the calibrators are weaker and therefore need to be observed for longer total integration times. Calibration every 20 minutes or so will often follow the longer-term atmospheric fluctuations at 20 cm and 6 cm, especially in the more compact VLA configurations. Calibration every 10 minutes or so is safer at 2 cm and 1.3 cm, especially if the external calibrator is within a degree or so of the target. It should not be necessary to calibrate instrumental effects more rapidly than every 30 minutes at 20 cm or 6 cm.

Finally, note the significance of the choice of the gain table interval for the VLA off-line data base created by the 'FILLER' program *if you will not self-calibrate* your data. The off-line gain table interval (which you specify to the array operator at the time of the observations) sets the minimum time scale of instrumental or atmospheric fluctuations that can be corrected by an external calibration. (Self-calibration algorithms construct their own gain tables based on the integration time τ_{sc} that you specify for the gain determination.) The VLA default gain table interval of 10 minutes is adequate for calibration under a stable atmosphere, but shorter intervals are often more appropriate if you will rely on external calibration.

b) Flux-density calibration.

If the LST range of your observing run permits, observe 3C 286 for a few minutes at each observing frequency used for the targets, as 3C 286 is the flux-density standard to which all VLA measurements are ultimately referred. Failing this, observe 3C 48 (or consult with VLA staff about recent determinations of the amplitude gains of the antennas from other observations before finalizing your observing program). Do not simply take the most recent flux density for an arbitrary calibrator from the *VLA Calibrator List*, as many small-diameter sources are variable. The flux densities recorded in the *VLA Calibrator List* will rarely have been measured recently enough to determine the absolute flux-density scale for your observations; use them only to estimate the integration times needed to achieve the desired gain accuracy from your calibrator scans.

c) Polarization calibration.

To calibrate the *instrumental polarizations*, observe one unresolved calibrator, whether polarized or not, at least three times. These observations should be distributed so they cover

a range in parallactic angle χ of $\Delta\chi \geq 90°$, to separate any polarization of the calibrator from the required instrumental terms (see Lecture 5). Programs involving long ($\geq$ 4 hr) syntheses of single sources will normally be able to derive the instrumental polarization calibration from the observations of the external gain calibrator. When determining the integration time for the instrumental polarization calibration, bear in mind that the leakage terms (the D's of Lecture 5) whose relative amplitudes and phases are to be determined will normally produce polarized intensities that are only a few percent of the flux density of the calibrator. The instrumental polarization calibration should be done at each frequency for which polarimetry is required. The most efficient way to do this is to cycle through the frequencies used for the target observations each time the array is pointed at the calibrator.

If the instrumental polarization calibration is omitted (e.g., because the observing session is too short, or the instrument misbehaved), you may be able to make the instrumental polarization corrections using the "standard" files of the necessary parameters that are maintained by the VLA staff. Note however that these are available only for a few combinations of observing frequency and bandwidth. If you omit an instrumental polarization calibration, you will be less able to determine small degrees of polarization, or to deconvolve polarized extended structures properly.[8]

To calibrate the *polarization position angle* scale, observe 3C 286 or 3C 138 at least once during your observing run at each relevant frequency. You will determine the apparent position angles of the linear polarization of these sources after you have finished observing and after calibrating the total intensity data. The difference between the apparent and the nominal values of these position angles is corrected by adjusting the phase difference between the left and right circular polarizations, using a procedure that is described in detail in the *VLA Cookbook*. It is advisable to alert the array operator to the presence of this calibration in your program, so that the observations of 3C 286 or 3C 138 can be extended or rescheduled if necessary to avoid losing them to equipment failure. Note that this calibration is *essential* if you wish to use your polarization position angle data.

At wavelengths of 18 cm and longer, the position angle calibration may appear to be time variable because of fluctuations in the ionospheric Faraday rotation (Lecture 5). If you will use the polarization position angle information at long wavelengths, it is worth monitoring one polarized calibrator *in the same part of the sky as your target(s)* throughout your observing, to see if its apparent position angle changes significantly. If this further calibration shows that the ionospheric changes are less than about 20°, it will probably be satisfactory to interpolate the observed position angle changes as a function of time when adjusting the relative phase of the left and right circularly polarized channels. If larger changes are seen, it may be possible to compensate for them using an ionospheric model and measured critical frequencies (by running the VLA's 'FARAD' program once the relevant critical frequency data have been received at the VLA—often several months after the observing). Except when the rotation changes are small ($< 20°$), the success of this repair cannot be guaranteed, however. The observation of the polarized calibrator can be a "warning light" for the existence of ionospheric Faraday rotation problems, not necessarily a means for correcting them. Applying FARAD's corrections to the data on this calibrator will also check whether they are indeed improving the angle calibration. Ionospheric effects will normally be negligible above about 4 GHz.

d) Self-calibration criteria.

To decide whether or not you will be able to self-calibrate VLA data, use Equation 24–4 with $N = 27$, i.e.,

$$\phi_{\rm rms} \approx \frac{13\Delta S}{S_{\rm sc}\sqrt{\Delta\nu\tau_{\rm sc}}} \text{ degrees}, \qquad \text{(24–A7)}$$

to estimate the phase error in a self-calibration interval $\tau_{\rm sc}$.

[8] Antenna-to-antenna polarization differences distort the polarization images in ways that do not satisfy the convolution theorem.

(19) Name	Epoch 1950☐ 2000☐ RA hh mm Dec -xx°x	Config.	Band (cm)	Band width (MHz)	Total Flux line (Jy)	Total Flux cont (Jy)	Largest ang size	Weakest signal (mJy/beam)	Required dynamic range	Possible LST range hh - hh	Time requested

Figure 24–6. A sample of Item 19 from the standard VLA proposal cover sheet.

e) Special problems of P Band.

Calibration at P Band is particularly troublesome because of confusion in the primary beam. Confusing sources contribute several Jy or more to every field of view, and the use of narrow bandwidths for interference rejection implies that these sources contribute significantly to virtually all baselines. External calibrators must therefore be chosen for their strength rather than by nearness to the interesting field of view. Calibrators with > 25 Jy are preferable. Unless the calibrator is > 5 Jy, you may as well attempt self-calibration using the brightest sources in the field. Self-calibration with the traditional algorithms may not work under severe ionospheric conditions, where the size of the isoplanatic patch may become smaller than that of the primary beam. Perley (1988) has listed possible P Band calibrators.

Because ionospheric Faraday rotation at P Band is large and variable, polarization calibration is extremely difficult and cannot be guaranteed unless the ionosphere is exceptionally "quiet" during an observing run.

A11. Observing Proposals

All VLA observing proposals are refereed outside the NRAO before being considered by the scheduling committee. To receive high priority, the scientific goals of the project must favorably impress the external referees. A "highly-placed source who wishes to remain anonymous" notes that more concisely-written proposals are more likely to be refereed favorably, all else being equal.

Before you begin writing a proposal, it is worth checking whether any of your target sources have already been observed at the VLA. The NRAO routinely archives the raw (uncalibrated) visibility data from all VLA observations. General access to these data is restricted for 18 months after the end of the associated observing program. Thereafter, the raw data are available to any scientist who adequately justifies their use. Calibrated and processed data remain the property of the original observer and are not automatically indexed or archived at the VLA. Full catalogs of the observed sources, including relevant instrumental parameters, can be obtained from Teresa McBride at the VLA, or by accessing the DEC-10 disk files ACCUM.SRT[13,542] (all observations > 1 hour) or yyyy.SRT[13,542] (all observations in year *yyyy*) on the VLA DEC–10 computer, or from the PC-based program 'VLASORS' (see below). If you decide that the major parameters of an earlier observation are also appropriate for your work, you may either contact the original observers to use their calibrated data, or request use of the uncalibrated data from the VLA archive. Watch the *NRAO Newsletter* for possible updates about the archive and associated software.

The proposal cover sheet should be filled out in as much detail as possible. Filling out item 19 on the cover sheet (Fig. 24–6) fully for each target, or for typical targets, will lead you to consider the issues discussed in this lecture. Your entries here should show the referees and the scheduling committee that the proposal is well suited to the requested configuration(s).

When writing the proposal, plan your calibration strategy in detail. The time you request should include all the on-source integration time that you need, plus time for any and all

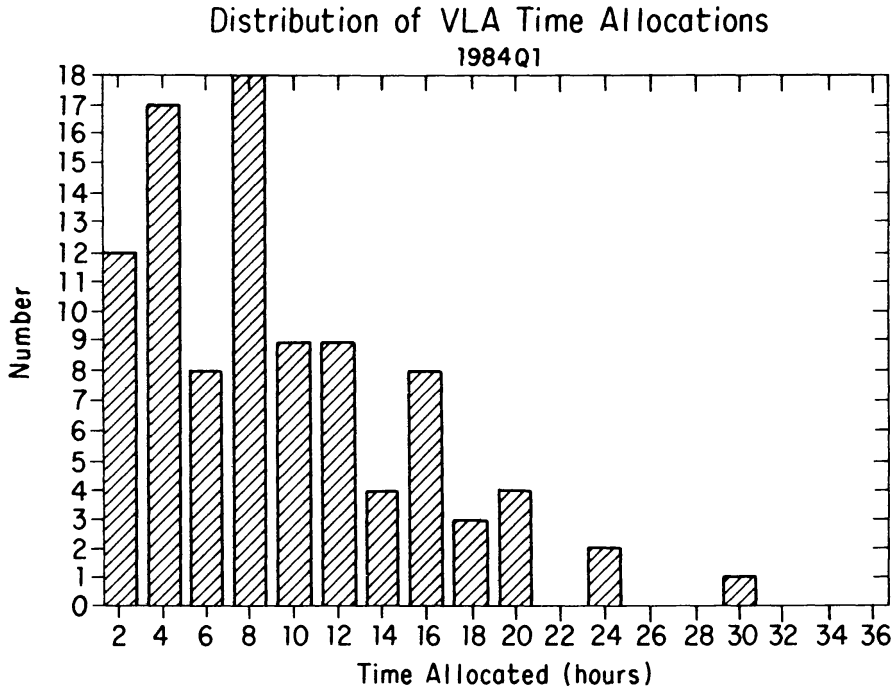

Figure 24–7. A histogram of durations of projects scheduled for VLA observations for the first two months of 1984, when the array was in the **B** configuration.

calibrations that you will do. Depending on the project, calibration time may need to be from 10% to 50% of the total request.

Figure 24–7 shows a typical histogram of the distribution of observing time allotted to successful VLA proposals. It covers the first two months of 1984, when the VLA was in the **B** configuration. The median observing time scheduled is 7 hours, reflecting how many proposals need less than full hour-angle tracks. Note however that some of the projects scheduled used more than 16 hours of observing time—well-justified long projects can successfully compete for time! The average number of proposals submitted to the VLA during 1983–87 was 466 per year, of which an average of 84 per year were rejected altogether. The average proposal scheduled received 55% of the requested observing time.

Proposals should be sent to the NRAO Director in Charlottesville well before the deadline for the desired configuration(s). The deadlines and the VLA configuration schedule are published regularly in the *NRAO Newsletter* and in the *AAS Newsletter*. Proposals may be submitted between the deadlines, and indeed the NRAO encourages this for several reasons—(a) the pressure of proposals for a given configuration influences the length of time that the VLA is scheduled to spend in that configuration, (b) early submission may let you reply to unfavorable referees' comments before the scheduling committee assigns time for the requested configuration(s), and (c) observers who submit early reduce the strain on the proposal processing system near the deadline.

A12. PC SOFTWARE

Two PC-based software packages that are useful when planning VLA observing can be obtained on request from Sandra Montoya at the NRAO in Socorro.

a) VLASORS.

This self-documenting database query program will search either for calibrators in the *VLA Calibrator List* or for sources from the observation archive list. The *Calibrator List* may be searched by source name, frequency, flux density, or area of sky. The archive list may be searched by source name, frequency, position, proposer or project number. 'VLASORS' can be run on any IBM PC or compatible computer with a hard disk. The archive of all observations

with total integration times longer than one hour requires 2.6 Mbytes of hard disk storage. The file of all observations requires 5 Mbytes. 'VLASORS' is distributed on three (> 60 min archive) or five (all observations) floppy diskettes.

b) VLAPLAN and VLAUVPL.

'VLAPLAN' (Bridle 1988) is a self-documenting, menu-driven spreadsheet that can be used to design continuum, spectral line, or bandwidth synthesis observing strategies for the VLA using the approaches and formulae described in this lecture. It organizes the relevant calculations into 'screens' that display the results of different parameter choices, offer advice on how to meet your imaging specifications within present VLA hardware and software limitations, and warn of parameter conflicts. 'VLAPLAN' also plots graphs of the bandwidth and time average smearing effects, of the primary beam correction, and of Gaussian source visibilities, scaled to the context of your parameter choices. It also warns of conflicts between the selected observing bandwidth and known interfering signals at L Band. 'VLAPLAN' requires an IBM PC or compatible with at least 320k of free RAM and a graphics board, and Lotus *1-2-3* (Version 2) or Borland *Quattro*.

'VLAPLAN' recommends VLA configuration(s) for your observing. It chooses the most compact configuration using only the observing frequency and the largest angular size and declination of your source. To save computation time, this recommendation is based on a table of the shortest projected baselines for *snapshots on the meridian* in each of the the four standard configurations, *at 10° intervals* in Declination. 'VLAUVPL' is an ancillary Lotus *1-2-3*, or *Quattro*, spreadsheet that computes the shortest projected baseline for *full synthesis* observations with the VLA at *any* Declination, but takes longer to run. It also generates u-v plots and graphs of $\sqrt{u^2+v^2}$ versus hour-angle over the full range of hour-angles consistent with your prescribed elevation limits, to help you plan short-baseline coverage in detail.

References

Adams, D. (1979), *The Hitch-Hiker's Guide to the Galaxy*, Pan Books, London.

Bridle, A. H. (1988), "VLAPLAN—VLA observing strategy planner", VLA Computer Memorandum No. 179, NRAO.

Clark, B. G. (1981), "Orders of magnitude of some instrumental effects", VLA Scientific Memorandum No. 137, NRAO.

Ledden, J. E., Broderick, J. J., Condon, J. J., and Brown, R. L. (1980), "A confusion-limited extragalactic source survey at 4.755 GHz. I. Source list and areal distributions", *Astron. J.*, **85**, 780–788.

Napier, P. J. and Rots, A. H. (1982), "VLA primary beam parameters", VLA Test Memorandum No. 134, NRAO.

Perley, R. A. (1981b), "VLA hybrid configuration u-v plane coverage", VLA Scientific Memorandum No. 139, NRAO.

Perley, R. A. (1988), "Calibration of P Band data", VLA Scientific Memorandum No. 159, NRAO.

Rots, A. H. (1988), *A Short Guide for VLA Spectral Line Observers (Edition 7.0)*, NRAO.

Sowinski, K. and Braun, R. (1988), "Interim spectral line support", VLA memorandum dated August 12, 1988, NRAO.

Thompson, A. R. (1982a), "The response of a radio-astronomy synthesis array to interfering signals", *IEEE Trans. Antennas Propagat.*, **AP-30**, 450–456.